THE JOURNAL OF BIOLOGICAL CHEMISTRY
Vol. 280, No. 19, Issue of May 13, pp. 18755–18770, 2005
Printed in U.S.A.

Statins Cause Intracellular Accumulation of Amyloid Precursor Protein, β-Secretase-cleaved Fragments, and Amyloid β-Peptide via an Isoprenoid-dependent Mechanism*

Received for publication, December 9, 2004, and in revised form, February 8, 2005
Published, JBC Papers in Press, February 17, 2005, DOI 10.1074/jbc.M413895200

Sarah L. Cole‡, Aneta Grudzien, Ingrid O. Manhart, Brent L. Kelly, Holly Oakley, and Robert Vassar§

From the Department of Cell and Molecular Biology, Northwestern University Medical School, Chicago, Illinois 60611

The use of statins, 3-hydroxy-3-methylglutaryl-CoA reductase inhibitors that block the synthesis of mevalonate (and downstream products such as cholesterol and nonsterol isoprenoids), as a therapy for Alzheimer disease is currently the subject of intense debate. It has been reported that statins reduce the risk of developing the disorder, and a link between cholesterol and Alzheimer disease pathophysiology has been proposed. Moreover, experimental studies focusing on the cholesterol-dependent effects of statins have demonstrated a close association between cellular cholesterol levels and amyloid production. However, evidence suggests that statins are pleiotropic, and the potential cholesterol-independent effects of statins on amyloid precursor protein (APP) metabolism and amyloid β-peptide (Aβ) genesis are unknown. In this study, we developed a novel *in vitro* system that enabled the discrete analysis of cholesterol-dependent and -independent (*i.e.* isoprenoid-dependent) statin effects on APP cleavage and Aβ formation. Given the recent interest in the role that intracellular Aβ may play in Alzheimer disease, we analyzed statin effects on both secreted and cell-associated Aβ. As reported previously, low cellular cholesterol levels favored the α-secretase pathway and decreased Aβ secretion presumably within the endocytic pathway. In contrast, low isoprenoid levels resulted in the accumulation of APP, amyloidogenic fragments, and Aβ likely within biosynthetic compartments. Importantly, low cholesterol and low isoprenoid levels appeared to have completely independent effects on APP metabolism and Aβ formation. Although the implications of these effects for Alzheimer disease pathophysiology have yet to be investigated, to our knowledge, these results provide the first evidence that isoprenylation is involved in determining levels of intracellular Aβ.

A growing body of evidence suggests that the amyloid β-peptide (Aβ)[1] plays a critical and early role in Alzheimer disease (AD) pathogenesis. AD is characterized by cerebral amyloid plaques, which are extracellular deposits of Aβ (1, 2). Overproduction of the 42-amino acid form of Aβ (Aβ42) is associated with early onset familial AD, and Aβ42 appears toxic to neurons *in vitro* and *in vivo* (reviewed in Refs. 3 and 4). Moreover, recent reports suggest that, in addition to extracellular Aβ, the accumulation of intracellular Aβ may be involved in AD (5–15). Thus, much research has been devoted to understanding the role of Aβ in AD and to developing therapeutic strategies for reducing Aβ levels or toxicity.

Aβ is cleaved from amyloid precursor protein (APP) by two proteases, the β- and γ-secretases (reviewed in Refs. 4, 16, and 17). Initially, β-secretase (also known as BACE1) cuts APP at the N terminus of the Aβ domain to produce the membrane-bound APP C-terminal fragment (CTF) C99 and the secreted APP ectodomain APPsβ. C99 is the substrate of γ-secretase, which cleaves to generate the C terminus of Aβ. γ-Secretase cleavage is heterogeneous and produces Aβ peptides of different lengths (~38–43 amino acids). An alternative non-amyloidogenic pathway also occurs in which a third protease, α-secretase, cuts APP within the Aβ domain, thus precluding Aβ formation. α-Secretase cleavage produces the membrane-bound APP CTF C83 and the secreted APP ectodomain APPsα. Like C99, C83 is a substrate of γ-secretase, which cleaves to generate the non-amyloidogenic p3 fragment. Previous studies indicate that the α- and β-secretase pathways may compete for APP substrate under certain conditions such that increased activity of one pathway leads to decreased APP processing in the other (18, 19).

Although Aβ42 is implicated as a causative factor for early onset familial AD, the link between Aβ and the pathogenesis of late onset sporadic AD is less firmly established. Factors that increase the risk of late onset AD have been identified, but their relationship to Aβ is unclear. Of particular interest are genetic and environmental factors that affect cholesterol metabolism and that associate with AD. For example, the apoE4 isoform is a risk factor for AD and is linked to increased serum cholesterol levels (20–22). Atherosclerosis and stroke, conditions that share hypercholesterolemia as a risk factor, appear to be associated with AD as well (23–26). Indeed, epidemiological studies indicate that

* This work was supported by Grant 53280004 from the Illinois Department of Public Health, Office of Health Promotion, and Grant IIRG-02-4282 from the Alzheimer's Association. The costs of publication of this article were defrayed in part by the payment of page charges. This article must therefore be hereby marked "*advertisement*" in accordance with 18 U.S.C. Section 1734 solely to indicate this fact.

‡ To whom correspondence may be addressed: Dept. of Cell and Molecular Biology, Feinberg School of Medicine, Northwestern University, 303 East Chicago Ave., Chicago, IL 60611. Tel.: 312-503-3700; Fax: 312-503-7912; E-mail: s-cole4@northwestern.edu.

§ To whom correspondence may be addressed: Dept. of Cell and Molecular Biology, Feinberg School of Medicine, Northwestern University, 303 East Chicago Ave., Chicago, IL 60611. Tel.: 312-503-3361; Fax: 312-503-7912; E-mail: r-vassar@northwestern.edu.

[1] The abbreviations used are: Aβ, amyloid β-peptide; AD, Alzheimer disease; APP, amyloid precursor protein; BACE, beta-site APP-cleaving enzyme; CTF, C-terminal fragment; APPs, secreted APP; HMG, 3-hydroxy-3-methylglutaryl; FPP, farnesyl pyrophosphate; GGPP, geranylgeranyl pyrophosphate; MβCD, methyl-β-cyclodextrin; FL-APP, full-length APP; LV, lovastatin; SV, simvastatin; LDFBS, lipoprotein-deficient fetal bovine serum; ELISA, enzyme-linked immunosorbent assay; APPsβsw, APPsβ with the Swedish mutation; DMEM, Dulbecco's modified Eagle's medium; FBS, fetal bovine serum; BisTris, 2-[bis(2-hydroxyethyl)amino]-2-(hydroxymethyl)propane-1,3-diol; ER, endoplasmic reticulum; TGN, *trans*-Golgi network.

high serum cholesterol levels increase the risk of AD, and it has been proposed that the homeostatic regulation of cholesterol metabolism may be altered in AD (27). In contrast, recent reports show a significant reduction in AD risk for patients treated with statins, a group of cholesterol-lowering drugs (28, 29). Taken together, these studies suggest that reduction of cholesterol levels may inhibit AD pathogenesis.

Statins are competitive inhibitors of 3-hydroxy-3-methylglutaryl (HMG)-CoA reductase, the enzyme that catalyzes the rate-limiting step in cholesterol biosynthesis (reviewed in Refs. 30 and 31). HMG-CoA reductase converts HMG-CoA into mevalonate (see Fig. 1*A*), and inhibition of HMG-CoA reductase reduces the synthesis of all mevalonate pathway products. Indeed, mevalonate is a precursor of not only cholesterol, but also of many nonsteroidal isoprenoids, including farnesyl pyrophosphate (FPP) and geranylgeranyl pyrophosphate (GGPP) (see Fig. 1*A*). Isoprenylation is a functionally important post-translational modification of a variety of proteins, including small GTPases (*e.g.* Ras, Rab, and Rho), and plays a crucial role in protein trafficking and signaling, cytoskeletal structure, cell motility, and membrane transport (32, 33). Thus, it has been postulated that statins may have significant cholesterol-independent effects that result from inhibition of the isoprenoid pathway.

Recent work has suggested that the AD risk reduction associated with statin treatment may be the result of decreased amyloidogenic APP processing caused by low cellular cholesterol levels. Treatment with statins or depletion of cholesterol with MβCD appears to increase α-secretase cleavage of APP in cells, whereas β-secretase cleavage and secreted Aβ levels are decreased (34–39). Conversely, cholesterol enrichment leads to elevated amyloidogenic processing of APP (40–42). Although these results suggest that cellular cholesterol levels modulate APP processing, other reports indicate that cholesterol esters (rather than free cholesterol) affect the activities of the secretases such that low cholesterol ester levels decrease Aβ formation (43). In addition, the subcellular distribution of cholesterol may also influence APP cleavage because mutations and pharmacological inhibitors of the Niemann-Pick complex cholesterol transport pathway alter the localization of presenilin/γ-secretase and lead to greater Aβ production (44–47). Thus, the form, level, and distribution of cholesterol in cells may modulate APP processing in a complex fashion.

Statins inhibit both cholesterol and isoprenoid synthesis, and therefore, it was important to determine their individual effects on APP processing because previous studies had not done so. To this end, in this work we investigated the cholesterol-dependent *versus* isoprenoid-dependent effects of statin treatment on APP cleavage and Aβ formation in cells. By independently manipulating total cellular cholesterol and isoprenoid levels during exposure to statins, we found that cholesterol and isoprenoids have differential effects on the secretion and intracellular accumulation of FL-APP, APP fragments, and Aβ. As expected from previous studies, low cellular cholesterol levels favor the α-secretase pathway and decrease Aβ secretion. However, we also obtained the novel result that low isoprenoid levels cause cell-associated accumulation of FL-APP, APP fragments, and intracellular Aβ, and these effects were reversed by supplementation with a low concentration of mevalonate or GGPP. Interestingly, low isoprenoid and cholesterol levels appear to act through unrelated mechanisms. In particular, the secreted and intracellular pools of Aβ behave independently of one another. Understanding both the cholesterol-dependent and isoprenoid-dependent statin effects on APP processing may shed light on the mechanisms involved in statin-mediated AD risk reduction and the accumulation of intracellular Aβ, which may play a role in AD pathophysiology.

EXPERIMENTAL PROCEDURES

Materials—The following reagents were used: lovastatin (LV) and simvastatin (SV) sodium salts (active forms; Calbiochem), lipoprotein-deficient fetal bovine serum (LDFBS) (Intracel), human Aβ40 and Aβ42 enzyme-linked immunosorbent assays (ELISAs) (BIOSOURCE International), ECL Plus (Amersham Biosciences), protease inhibitor cocktail (Calbiochem), and BCA protein assay (Pierce). All chemicals were obtained from Sigma unless specified otherwise. Rabbit antisera against APP amino acids 676–695 and APPsβ with the Swedish mutation (APPsβsw) were generated as described (18). Other antibodies used were anti-APP antibody 22C11 (Chemicon International, Inc.), anti-Aβ-(1–17) antibody 6E10 (Signet Laboratories, Inc.), anti-BACE1 antibody PA1-757 (Affinity Bioreagents), anti-β-tubulin III antibody TUJ1 (Covance), anti-glial fibrillary acidic protein antibody G-A-5 (Sigma), anti-actin antibody AC-15 (Sigma), peroxidase-conjugated secondary antibodies (Jackson ImmunoResearch Laboratories, Inc.), and fluorescein 5-isothiocyanate-conjugated secondary antibodies (Vector Laboratories).

Cell Line Culture and Adenovirus Infection—HEK293 cells expressing human APP695 containing the Swedish mutation (APPsw-293 cells) were generated as described (48) and cultured in high glucose Dulbecco's modified Eagle's medium (DMEM), 10% fetal bovine serum (FBS), 400 μg/ml G418, 5 μg/ml puromycin, and 1% penicillin/streptomycin. Human SH-SY5Y neuroblastoma cells were cultured in high glucose DMEM, 10% FBS, and 1% penicillin/streptomycin. Recombinant adenovirus encoding human APP695sw was prepared as described previously (49). Prior to drug treatment, SH-SY5Y cells were infected for 48 h with APP695sw adenovirus.

Neuron Culture—Primary cultures of cortical neurons were prepared from day 15–16 Tg2576 mouse embryos as described (50). Briefly, embryo cortices were dissected, and meninges were removed. Tissue was digested with 0.25% trypsin, mechanically dissociated, suspended in neurobasal medium (supplemented with 10% horse serum, B27 supplement, 100 μg/ml penicillin/streptomycin, 0.5 mM glutamine, and 25 μM glutamate), and plated densely onto poly-D-lysine-coated 6-well plates. Neurons were maintained under serum-free conditions in neurobasal medium with B27 supplement prior to drug treatment. The neuronal population was determined to be >95% pure by immunofluorescence microscopy using β-tubulin III immunoreactivity as a neuronal marker.

Astrocyte Culture—Primary mouse astrocytes were prepared from Tg2576 P1 pups. Briefly, P1 cerebral cortices were dissected, and the meninges were removed. Tissue was digested with 0.25% trypsin; gently dissociated; suspended in low glucose DMEM, 10% FBS, and 1% penicillin/streptomycin; and either plated onto poly-D-lysine-coated 6-well plates for experimentation after 5 days *in vitro* (primary astrocytes) or seeded into T75 flasks (secondary astrocytes). To establish a pure astrocyte culture, microglia were removed by shaking at 275 rpm for 1 h at 37 °C. At confluence, astrocytes were split and seeded onto poly-D-lysine-coated 6-well plates at a density of $\sim 2 \times 10^5$ cells/well (secondary astrocytes). The astrocyte population was determined to be >95% pure by immunofluorescence microscopy using glial fibrillary acidic protein immunoreactivity as an astrocyte marker. Experiments were performed using both primary and secondary astrocyte cultures, and similar effects on APP metabolism were observed in both cases. For neuronal and astrocyte cultures, genotype analysis was performed with a REDExtract-N-Amp™ tissue PCR kit (Sigma) using Tg2576 transgene primers as described (51).

Statin and MβCD Treatments—24 h prior to treatment, APPsw-293, SH-SY5Y, and astrocyte cells were seeded onto poly-D-lysine-coated 6-well plates at a density to obtain subconfluent cell monolayers at the time of drug treatment. For Aβ ELISAs, cells were plated onto 10-cm dishes. Cultures were then treated with LV or SV (see "Results" for details on concentrations and treatment times) in the presence or absence of 0.25 mM mevalonate (34, 37, 38, 52). Drug treatments were performed in triplicate, and experiments were repeated four times. Cell viability (as determined by trypan blue exclusion) remained above ~95% following drug exposure. Statins were applied to APPsw-293, SH-SY5Y, and astrocyte cultures in DMEM containing either 10% FBS or 10% LDFBS. For treatment of primary cortical neurons, statins were applied under serum-free conditions in neurobasal medium with B27 supplement. As an alternative method to lower cellular cholesterol levels, APPsw-293 cells were treated with 10 mM MβCD in either FBS- or LDFBS-containing DMEM for 30 min at 37 °C. The MβCD-containing medium was then removed, and cells were maintained in serum-free medium for 3.5 h before harvest. MβCD treatments were performed in triplicate, and experiments were repeated three times.

Immunoblot Analysis—Following treatment, the conditioned media were harvested, and cells were scraped into lysis buffer (20 mM Tris-HCl (pH 6.8), 2% SDS, 5% glycerol, and 0.01% sodium azide) with protease inhibitor cocktail, and the protein concentration was measured with using the BCA protein assay kit. Equal amounts of protein (20 μg/lane for detection of APP CTFs and 10 μg/lane for all other proteins) were boiled under reducing conditions, loaded onto either NuPAGE 4–12% BisTris gels or 18% Tris/glycine gels (Novex and Invitrogen), and transferred to polyvinylidene difluoride membrane. For FL-APP, C99, and C83 detection, blots were probed with anti-APP-(676–695) antiserum (1:5000). In addition, FL-APP was also detected by immunoblot analysis using either antibody 22C11 (1:10,000) or 6E10 (1:10,000; which predominantly detects FL-APP in cell lysates). For detection of APPsα and APPsβsw, blots were probed with antibody 6E10 (1:10,000) and anti-APPsβsw antiserum (1:5000), respectively. For BACE1 detection, antibody PA1-757 (1:1000) was used. Blots were co-incubated with anti-β-actin antibody (1:10,000) to control for loading. Following application of peroxidase-conjugated secondary antibodies, immunoblot signals were detected by enhanced chemiluminescence using ECL Plus and quantified using a Kodak Image Analyzer (440 CF). All drug treatments were carried out in triplicate, and signals are expressed as a percentage of the control ± S.E. following signal normalization relative to the β-actin signal of each sample.

Quantitative Real-time Reverse Transcription-PCR—APPsw-293 cells were exposed to either vehicle (untreated control) or 1–10 μM LV for 48 h. Total RNA was isolated (SV total RNA isolation kit, Promega), and cDNA was generated (Advantage RT-for-PCR kit, Clontech). Quantitative PCR was performed on an Applied Biosystems Prism 7900 sequence analyzer using LightCycler-FastStart DNA Master SYBR Green I (Roche Applied Science) with 0.3 μM each primer, 1.5 mM $MgCl_2$, and 50 ng of cDNA. PCR cycle parameters were 50 °C for 2 min and 95 °C for 10 min, followed by 40 cycles at 95 °C for 15 s and 60 °C for 1 min. Following the final cycle, melt curve analysis confirmed the specificity and purity of each PCR product. Primer sequences were as follows: human β-actin forward primer, TCC CTG GAG AAG AGC TAC GA; actin reverse primer, AGC ACT GTG TTG GCG TAC AG; human APP695 forward primer, TGG CCC TGG AGA ACT ACA TC; and APP reverse primer, AAT CAC ACG GAG GTG TGT CA. Samples were run in triplicate; data were analyzed using a relative quantification method (Applied Biosystems); and β-actin values were used for signal normalization.

Immunocytochemistry—Cells were fixed in 4% paraformaldehyde, permeabilized with Triton X-100, and prepared for immunofluorescence microscopy as described (18). The primary antibodies used were anti-APP-(676–695) antiserum (1:100), anti-APPsβsw antiserum (1:750), anti-β-tubulin III antibody (1:250), and anti-glial fibrillary acidic protein antibody (1:400), and the secondary antibody used was fluorescein 5-isothiocyanate-conjugated antibody (1:400).

Total Cholesterol Level Determination—Total lipids were extracted from cells according to established procedures (53). Briefly, APPsw-293 cells (~5×10^6 cells) were scraped from 10-cm dishes, transferred to microcentrifuge tubes, washed twice with ice-cold phosphate-buffered saline, and centrifuged at 7000 × *g* for 10 min. Pellets were resuspended in 0.5 ml of isopropyl alcohol, sonicated for 2.5 min, and cleared by centrifugation at 10,000 × *g* for 10 min. Supernatants were decanted; the isopropyl alcohol was evaporated; pellets were resuspended in ~50 μl of isopropyl alcohol; and aliquots were taken for cholesterol analysis. The cholesterol level was measured using a total cholesterol determination kit (Sigma) with cholesterol standards used for calibration according to the manufacturer's directions. Results were normalized to the total protein concentration of each sample. Treatments were performed in triplicate; the experiment was repeated three times; and the results are reported as a percentage of the control ± S.E.

Quantification of Cell-associated and Secreted Aβ Levels—Following drug treatments, the culture medium was collected, supplemented with protease inhibitor cocktail, and centrifuged at 16,000 × *g* for 5 min at 4 °C. 100 μl of supernatant was used for Aβ40 and Aβ42 quantification by colorimetric sandwich ELISA according to the BIOSOURCE protocol. The protein concentration of the remaining supernatant was determined by BCA assay following overnight trichloroacetic acid precipitation. To measure cell-associated Aβ40 and Aβ42, cells were washed twice with cold phosphate-buffered saline, and cell pellets (~50 μl) were solubilized in 125 μl of cold 5 M guanidine HCl and 50 mM Tris-HCl (pH 8.0). Following a brief sonication, samples were mixed at room temperature for 4 h, diluted into cold Dulbecco's phosphate-buffered saline with 5% bovine serum albumin and 0.03% Tween 20 supplemented with protease inhibitor mixture (final guanidine HCl concentration of 0.1 M), and cleared by centrifugation at 16,000 × *g* for 20 min at 4 °C. Cell-associated Aβ40 and Aβ42 concentrations were measured by ELISAs as described above using 100 μl of the supernatant. The ELISAs are incompatible with guanidine concentrations >0.1 M, and at this dilution, the level of cell-associated Aβ42 fell below the detection limits of the ELISA. Treatments were performed in triplicate, and the quantity of Aβ in each sample was measured in duplicate. Data are expressed in three ways: (i) as total Aβ (nanograms ± S.E.; nanograms/ml multiplied by the total volume, 5 ml of medium or 0.175 ml of cell lysate), (ii) as Aβ concentration (nanograms/ml ± S.E.) in the medium and within the cell (total cell-associated Aβ divided by the cell pellet volume, 50 μl), and (iii) cell-associated Aβ levels normalized to total protein content in the cell lysate and expressed as a percentage of the vehicle control ± S.E. and secreted Aβ levels expressed as a percentage of the vehicle control ± S.E.

RESULTS

Experimental Strategy for Analyzing Cholesterol-dependent Versus Isoprenoid-dependent Effects on APP Processing—Total cellular cholesterol levels are maintained by a combination of cholesterol biosynthesis in the endoplasmic reticulum (ER) (Fig. 1*A*) and receptor-mediated endocytosis of cholesterol-containing lipoprotein particles (reviewed in Refs. 54 and 55). In the event that one of these two cholesterol pathways is blocked, the other pathway is capable of maintaining normal cholesterol levels within the cell. For example, if cholesterol biosynthesis is inhibited by treatment with statin drugs, then cells may obtain cholesterol via low density lipoprotein receptor-mediated uptake of lipoprotein particles from the medium. Conversely, if the medium is deficient in lipoprotein particles, then the cell may generate cholesterol endogenously through the biosynthetic pathway involving HMG-CoA reductase.

In the cholesterol biosynthetic pathway, statin-induced inhibition of HMG-CoA reductase blocks the synthesis of mevalonate and all downstream products, including both cholesterol and the nonsterol isoprenoids (Fig. 1*A*). As noted previously, the major cholesterol-independent effects of the statins are likely due to inhibition of isoprenoid pathways (30, 31). Studies have shown that statin-induced blockade of isoprenoid biosynthesis may be abrogated by adding low concentrations (~0.25 mM) of mevalonate to the culture medium during statin treatment (34, 37, 38, 52, 54–56). Importantly, under these conditions of statin plus low mevalonate, cholesterol production remains insignificant, whereas isoprenoid function is rescued.

We have exploited these properties of the cholesterol and isoprenoid pathways to develop an experimental strategy for manipulating cellular cholesterol and isoprenoid levels independently of one another (Fig. 1, *B–F*). With this strategy, we have been able to analyze the cholesterol-dependent *versus* isoprenoid-dependent effects of statin treatment on APP processing in cells. As a model cell culture system, we used HEK293 cells stably transfected with human APP695 containing the Swedish mutation (APPsw-293 cells). APPsw-293 cells are technically facile and have been used extensively to analyze APP processing. We investigated statin effects under four conditions: Condition 1, normal cholesterol and low isoprenoid levels (Fig. 1*C*); Condition 2, low cholesterol and low isoprenoid levels (Fig. 1*D*); Condition 3, normal cholesterol and normal isoprenoid levels (Fig. 1*E*); and Condition 4, low cholesterol and normal isoprenoid levels (Fig. 1*F*). In Condition 1, cells are treated with statins in medium containing FBS, which is rich in cholesterol-containing lipoprotein particles (Fig. 1*C*), so both cholesterol and isoprenoid biosynthesis are blocked, but normal cellular cholesterol levels are maintained by low density lipoprotein receptor-mediated endocytosis. On the other hand, cells cultured with statins in LDFBS (Condition 2) (Fig. 1*D*) can not obtain cholesterol by endocytosis, and they are not capable of synthesizing cholesterol or isoprenoids due to HMG-CoA reductase inhibition. In this case, cells experience depressed levels of both cholesterol and isoprenoids. In Condition 3, supplementation of statin-treated cells with 0.25 mM meva-

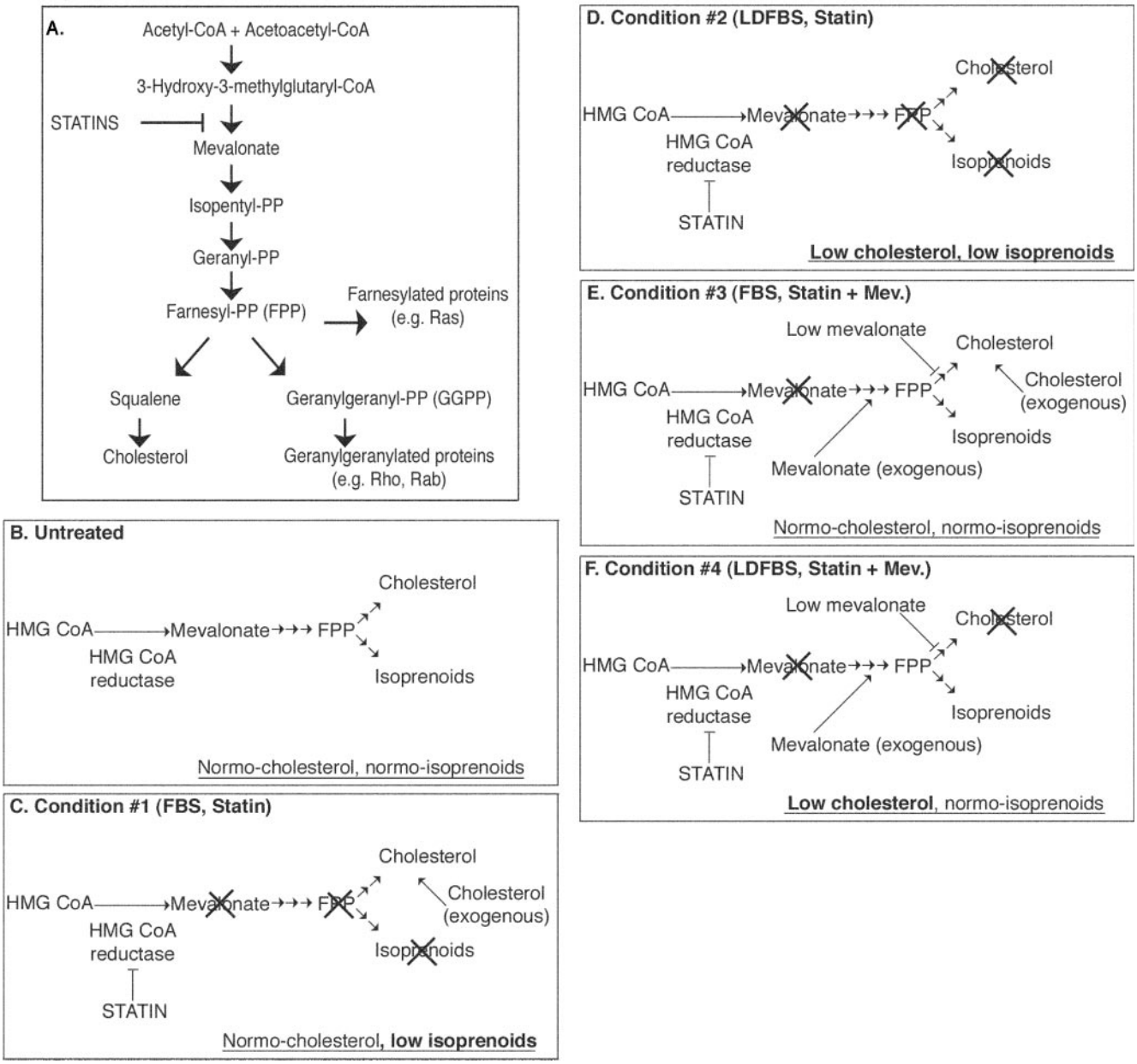

FIG. 1. **Cholesterol biosynthetic pathway and experimental strategy.** *A*, statin-induced inhibition of HMG-CoA reductase in the ER blocks the synthesis of mevalonate and all downstream intermediates, including cholesterol and nonsterol isoprenoids such as FPP and GGPP. *PP*, pyrophosphate; *Normo*, normal. *B*, in untreated cells, normal cholesterol and normal isoprenoid levels are maintained by the activities of the cholesterol biosynthetic pathway and receptor-mediated endocytosis of cholesterol-containing lipoprotein particles. *C* (Condition 1), in a cholesterol-rich environment (FBS-containing medium), cells maintain normal cholesterol levels by uptake of exogenous cholesterol, but experience low isoprenoid levels due to statin-induced inhibition of mevalonate. *D* (Condition 2), cells maintained in LDFBS-containing medium lack a source of exogenous cholesterol, so application of statin under these conditions leads to a depression of both cellular cholesterol and isoprenoid levels. *E* (Condition 3), low concentrations of exogenous mevalonate (*Mev.*) rescue statin-induced isoprenoid inhibition (without significantly contributing to total cholesterol levels), and cells take up exogenous cholesterol from FBS-containing medium to maintain both normal cholesterol and normal isoprenoid levels. *F* (Condition 4), in LDFBS-containing medium, cells lack an external source of cholesterol, and low levels of exogenous mevalonate rescue statin-induced blockade of isoprenoid synthesis, so cells experience low cholesterol and normal isoprenoid levels.

lonate in FBS-containing medium circumvents the statin-induced blockade of isoprenoid synthesis, and cells maintain normal cholesterol levels by endocytosis of FBS-derived lipoprotein particles (Fig. 1*E*). In Condition 4, statin-treated cells in LDFBS plus 0.25 mM mevalonate have normal isoprenoid levels due to mevalonate supplementation, but do not have a source of cholesterol from the medium and therefore experience depressed cholesterol levels (Fig. 1*F*). As a complementary method to examine the effects of cholesterol reduction on APP processing, total cellular cholesterol levels were lowered by treating cells with MβCD, which has been shown to selectively and rapidly extract cholesterol from the plasma membrane in preference to other lipids (34, 57).

To verify that we could independently manipulate cellular cholesterol and isoprenoid levels with our experimental strategy, APPsw-293 cells were treated according to the conditions outlined above, and total cellular cholesterol levels were measured using a cholesterol assay. As expected from previous studies (34, 37, 52), cell viability following treatment under all conditions was >95% as determined by trypan blue staining (data not shown). Exposure of APPsw-293 cells to either 10 mM MβCD for 30 min or 10 μM LV for 24 h in LDFBS-containing

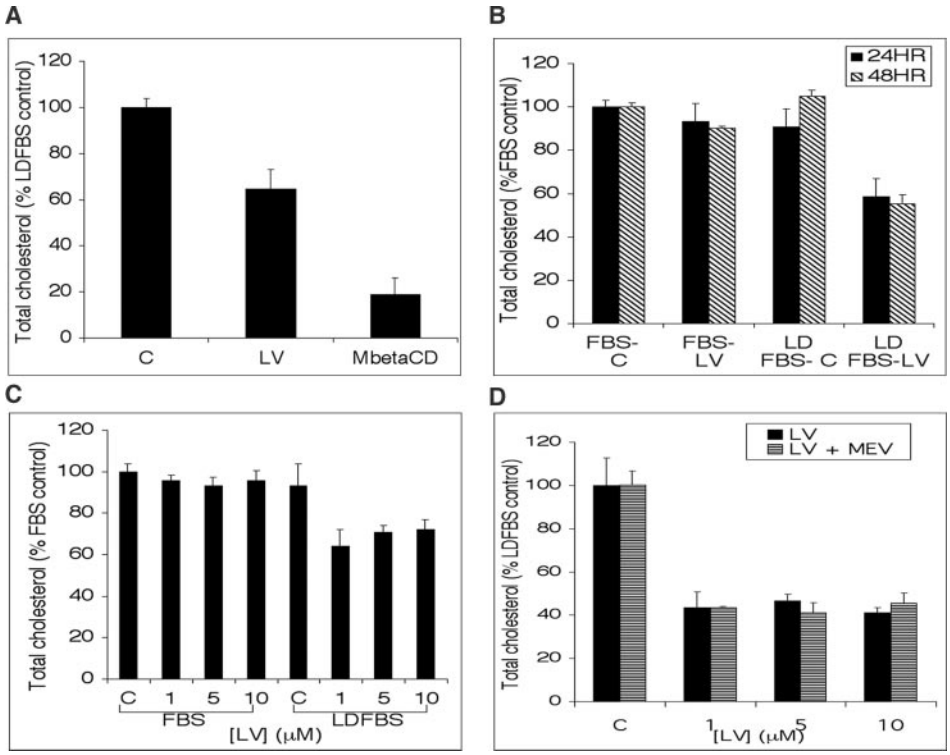

FIG. 2. **Statin reduces total cholesterol levels only in the absence of exogenous cholesterol.** 0.25 mM mevalonate did not rescue statin-induced depression of cellular cholesterol. Following treatment, the total cellular cholesterol content of APPsw-293 cells was measured by cholesterol assay. *A*, cells were exposed to vehicle (control (*C*)), 10 μM LV for 24 h in LDFBS (*LV*), or 10 mM MβCD for 30 min (*MbetaCD*). *B*, cells were maintained in either FBS or LDFBS and exposed to vehicle (*FBS-C* and *LDFBS-C*) or 10 μM LV (*FBS-LV* and *LDFBS-LV*) for 24 or 48 h. *C*, cells were maintained in either FBS or LDFBS and exposed to vehicle or the indicated concentrations of LV for 48 h. *D*, cells were maintained in LDFBS and exposed to vehicle or the indicated concentrations of LV in the absence or presence of 0.25 mM mevalonate (*MEV*) for 48 h. Note that reductions in cellular cholesterol were observed only following application of statin to cells maintained in LDFBS-containing medium and that similar reductions in cellular cholesterol were observed following statin treatment in the absence or presence of mevalonate. Data are representative and are expressed as a percentage of the control ± S.E.

medium reduced the total cellular cholesterol content to ~20 and ~60%, respectively, of the cholesterol levels found in control cells grown in LDFBS plus vehicle (Fig. 2*A*). The cells treated with LV in LDFBS-containing medium correspond to Condition 2, in which both cholesterol and isoprenoid levels are depressed (Fig. 1*D*). As anticipated, APPsw-293 cells treated with LV in FBS-containing medium, corresponding to Condition 1, did not show significantly reduced cholesterol levels compared with control cells cultured in FBS-containing medium plus vehicle even when cells were exposed to LV at concentrations up to 10 μM and for times as long as 48 h (Fig. 2, *B* and *C*). Cells incubated with LV in FBS-containing medium have normal cholesterol levels as a result of cholesterol uptake from the medium, but have depressed isoprenoid levels due to statin-induced inhibition of mevalonate biosynthesis (Fig. 1*C*).

LV treatment of cells in LDFBS caused approximately the same amount of cholesterol reduction at all doses and times tested (Fig. 2, *B–D*). Importantly, addition of 0.25 mM mevalonate to cells treated with LV in LDFBS-containing medium did not increase total cholesterol levels compared with those of cells exposed to LV alone in LDFBS (Fig. 2*D*), indicating that supplementation with a low concentration of mevalonate does not significantly rescue the statin-induced inhibition of cholesterol biosynthesis. This corresponds to Condition 4, in which statin-treated cells experience low total cholesterol levels as a result of cholesterol biosynthesis inhibition and lipoprotein-deficient medium, but have normal isoprenoid levels due to mevalonate supplementation (Fig. 1*F*). As predicted, LV-treated cells in FBS-containing medium plus 0.25 mM mevalonate had control levels of total cholesterol (data not shown), corresponding to Condition 3, in which cellular cholesterol and isoprenoid levels are normal (Fig. 1*E*). Taken together, these results demonstrate that we were able to individually manipulate cellular levels of cholesterol and isoprenoids, and thus, we can dissect cholesterol-dependent and isoprenoid-dependent effects of statins on APP processing.

Statins Induce the Accumulation of Cell-associated β-Secretase-cleaved APP Fragments and Intracellular Aβ in a Cholesterol-independent Manner—To investigate the cholesterol-dependent and isoprenoid-dependent effects of statins on APP processing, we treated APPsw-293 cells with different concentrations of LV and SV in FBS- or LDFBS-containing medium with or without 0.25 mM mevalonate for 48 h. We then harvested cell lysates and conditioned media and performed immunoblot analysis for FL-APP and cleaved APP fragments, including APPsα, APPsβ, C83, and C99. In addition, we measured Aβ40 and Aβ42 levels in cell lysates and conditioned media by specific sandwich ELISAs.

Using antibodies 22C11 and 6E10 and anti-APP-(676–695) antiserum, immunoblot analysis of cell lysates showed a dose-dependent increase in the levels of FL-APP and APP-derived fragments upon statin treatment (Fig. 3, *A*, *D*, *F*, *G*, and *I*). Although anti-APP-(676–695) immunoblots needed to be over-exposed to visualize APP CTFs (Fig. 3, *A–F*, *upper panels*), lower exposures revealed statin-induced increases in FL-APP levels (Fig. 3*I*, *middle panel*). Similar results were obtained following immunoblot analysis with antibodies 22C11 (Fig. 3, *A*, *D*, and *F*, *middle panels*; and *I*, *upper panel*) and 6E10 (Fig. 3*I*, *lower panel*), which recognize the APP ectodomain and Aβ-(1–17), respectively. It has been reported previously that antibody 22C11 recognizes an APP homolog, APP-like protein, in addition to APP (58). In contrast, antibody 6E10 is specific

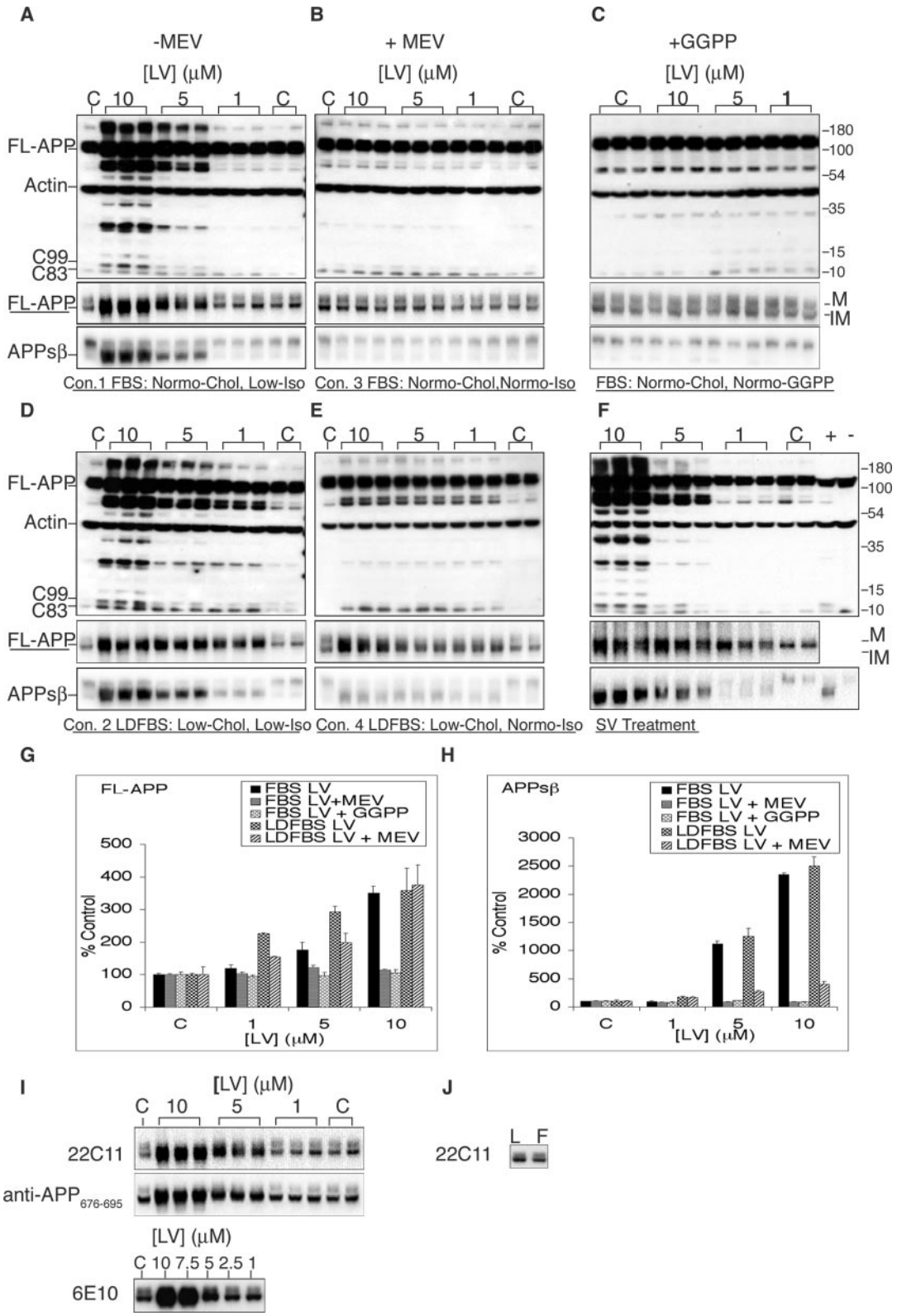

FIG. 3. **Statin treatments induce the accumulation of cell-associated APP and β-secretase-cleaved APP fragments in an isoprenoid-dependent manner.** APPsw-293 cells were treated with vehicle (control (C)) or the indicated concentrations of LV (*A–E* and *I*) or SV (*F*) for 48 h in FBS (*A–C*, and *F*, *upper panel*; and *I*) or LDFBS (*D*, *E*, and *F*, *middle* and *lower panels*). Some cultures were supplemented with 0.25 mM mevalonate (*MEV*) (*B* and *E*) or 10 μM GGPP (*C*). Following treatment, cell lysates were prepared and analyzed by immunoblotting with anti-APP-(676–695) antiserum plus anti-actin antibody (*A–F*, *upper panels*), antibody 22C11 (FL-APP) (*A–F*, *middle panels*; and *I*, *upper panel*), anti-APPsβsw antiserum (*A–F*, *lower panels*), or antibody 6E10 (*I*, *lower panel*). Note that LV and SV treatments caused a dose-dependent increase in the levels of cell-associated FL-APP and β-secretase-cleaved APP fragments and that supplementation with mevalonate or GGPP inhibited these increases. Similar effects were observed for 24-h treatments (not shown). For the identification of APPsβ and C83 and C99 CTFs, + and − *lanes* in *F* were loaded with cell lysates from APPsw adenovirus-infected mouse neurons with wild-type (+) or BACE1$^{-/-}$ (−) genotypes. Comparison of the + and − *lanes* confirmed the identity of APPsβ (*F*, *lower panel*) and C99 (*upper panel*, + *lane*; ~12-kDa band). Molecular mass markers (in kilodaltons) are shown on the right, as are the positions of mature (*M*) and immature (*IM*) APP. Under the *lower panels* in *A–F* are the conditions (*Con.*) described under "Results." *Normo*, normal; *Chol*, cholesterol; *Iso*, isoprenoids. The immunoblots for the LV experiment were scanned on a

for APP only. Because antibody 6E10 showed similar dose-dependent increases in immunoreactivity compared with antibody 22C11 and anti-APP-(676–695) antiserum, we concluded that signals from all three anti-APP antibodies predominantly represented levels of FL-APP rather than APP-like protein.

Both LV and SV appeared to have similar dose-response effects on FL-APP accumulation in cells maintained in either FBS or LDFBS (Fig. 3, compare *A* and *D* with *F*). Interestingly, the dose-response nature of statin treatment on APP levels contrasted with the absence of a dose-response relationship of statin treatment with total cholesterol levels (Fig. 2, *C* and *D*). Furthermore, increased FL-APP levels were observed for statin-treated cells maintained in either FBS-containing medium (Fig. 3, *A*, *F*, and *I*) or LDFBS-containing medium (Fig. 3*D*), indicating that the statin-induced accumulation of APP occurred regardless of whether total cellular cholesterol levels were normal (FBS; Condition 1) or low (LDFBS; Condition 2). As we will demonstrate below, these effects are not related to cellular cholesterol levels, but instead are due to low levels of isoprenoids in the cell.

Using the antibody 22C11 immunosignal for quantification, at the highest LV dose (10 μM), the value of the FL-APP level reached ~400% of that found in vehicle-treated control cells (Fig. 3*G*). The anti-APP antibodies detected bands on immunoblots of ~110 and ~130 kDa that have been identified previously as immature APP and mature APP, respectively (59, 60). Notably, statin treatment appeared to elevate the level of immature APP to a greater extent than that of mature APP (FL-APP) (Fig. 3, *A*, *D*, and *I*), suggesting that the bulk of APP accumulation occurred within early biosynthetic compartments.

Our results suggested that statin treatment caused the post-translational accumulation of APP within the cell, although it was also possible that the increased APP levels may have been due to statin-stimulated up-regulation of APP transgene expression or APP mRNA stabilization. To test this hypothesis, we performed quantitative reverse transcription-PCR using APP-specific primers to amplify RNA isolated from LV-treated and control APPsw-293 cells. We found that APP mRNA levels in statin-treated cells were similar to those found in vehicle control cells (data not shown), demonstrating that the APP increase was not due to an effect of statins on APP transgene expression or mRNA stability.

Immunoblot analysis with anti-APP-(676–695) antiserum also identified the α- and β-secretase-cleaved CTFs of APP, C83, and C99, respectively. We observed that the levels of C99 (~12 kDa) increased with LV and SV treatment in a dose-dependent manner (Fig. 3, *A*, *D*, and *F*, *upper panels*), thus paralleling the rise in FL-APP levels. This C99 increase occurred regardless of whether cells were treated in FBS-containing medium (Fig. 3, *A* and *F*) or LDFBS-containing medium (Fig. 3*D*). In contrast, the level of C83 (~10 kDa) in FBS-grown cells was not substantially raised following treatment (Fig. 3, *A* and *F*), whereas C83 levels were significantly elevated over control levels in statin-treated LDFBS-maintained cells (Fig. 3*D*). Interestingly, this C83 increase had approximately the same value for all LV doses (Fig. 3*D*) and was inversely correlated with the dose-independent decrease in total cholesterol levels following LV treatment in LDFBS (Fig. 2, *C* and *D*). In addition to the rise in C99 and C83 levels, statin treatment also increased the levels of at least six unidentified APP C-terminal immunoreactive bands ranging in size from ~15 to >180 kDa on blots incubated with anti-APP-(676–695) antiserum (Fig. 3, *A*, *D*, and *F*). Further investigation will be required to fully characterize these additional APP-derived CTFs.

The elevated level of C99 implied that the other β-secretase cleavage product, APPsβ, might also be increased following statin treatment. To investigate this possibility, we immunoblotted the lysates from statin-treated APPsw-293 cells and incubated the blots with antiserum directed against the free C terminus of APPsβsw generated after β-secretase cleavage. This neoepitope antibody has high affinity for the cleaved APPsβsw ectodomain, but only very weakly cross-reacts with FL-APPsw (Fig. 3*F*, *lower panel*, compare + and − *lanes*). As predicted from the rise in C99 levels, immunoblot analysis of cell lysates using anti-APPsβsw antiserum revealed that levels of cell-associated APPsβ increased in a dose-dependent manner following exposure to either LV or SV (Fig. 3, *A*, *D*, and *F*, *lower panels*). Moreover, the statin-induced APPsβsw increase was dramatic, reaching ~2500% of control cell levels for 10 μM LV (Fig. 3*H*), and occurred regardless of whether cells were treated in FBS- or LDFBS-containing medium. The apparent accumulation of APPsβ within the cell is atypical because APPsβ is normally efficiently secreted into the extracellular medium, and very little APPsβ remains cell-associated.

To directly establish whether the large increase in cell-associated APPsβ detected by immunoblotting was the result of APPsβ accumulation within intracellular compartments, we performed indirect immunofluorescence microscopy on LV-treated APPsw-293 cells following incubation with anti-APPsβsw antiserum (Fig. 4*B*). As expected, a robust anti-APPsβsw signal was observed within subcellular compartments in statin-treated cells (Fig. 4*B*), demonstrating that the increase in the levels of cell-associated APPsβ was indeed the result of intracellular accumulation.

The high levels of amyloidogenic C99 and intracellular APPsβ indicated that β-secretase cleavage of APP increased in cells following statin treatment, and therefore, it appeared likely that Aβ levels could also be elevated in response to statins. To investigate this possibility, we treated APPsw-293 cells with LV in FBS or LDFBS as described above and analyzed cell lysates for levels of intracellular Aβ40 and Aβ42 by specific sandwich ELISAs. As observed for the levels of FL-APP and β-secretase-cleaved APP fragments, statin treatment in either FBS- or LDFBS-containing medium caused a dose-dependent increase in Aβ40 levels within the cell (Fig. 5, *A–C*). Cell-associated Aβ42 was below the level of detection in the Aβ42-specific ELISA for the doses and times of LV treatment tested (data not shown). We also noted that untreated cells maintained in LDFBS exhibited cell-associated Aβ40 levels that were slightly lower than those observed in cells maintained in FBS. In addition, the LV-induced increases in cell-associated Aβ40 levels appeared muted in cells maintained in LDFBS compared with those in FBS (Fig. 5, *A* and *B*). However, following normalization of Aβ40 levels to cellular protein content, the magnitudes of the cell-associated Aβ40 increases in cells grown in either FBS or LDFBS were approximately the same, reaching

PhosphorImager, and immunoreactive signals for FL-APP (sum of mature and immature APP band signals) obtained with antibody 22C11 (*G*) and APPsβ (*H*) were quantified and normalized against actin and are expressed as a percentage of the control ± S.E. Cell lysates from the experiment in *A* were rerun on duplicate gels and analyzed by immunoblotting with antibody 22C11 (*I*, *upper panel*) and anti-APP-(676–695) antiserum (*middle panel*). In a separate experiment, lysates from LV-treated cells were analyzed by immunoblotting with antibody 6E10 (*lower panel*). Blot exposures were approximately matched to demonstrate that all three antibodies revealed similar LV dose-dependent increases in FL-APP levels. Lysates from vehicle-control cells maintained in LDFBS (*L*) or FBS (*F*) were analyzed by immunoblotting with antibody 22C11 to show that FL-APP levels were the same in cells grown in either lipoprotein-deficient or normal serum (*J*).

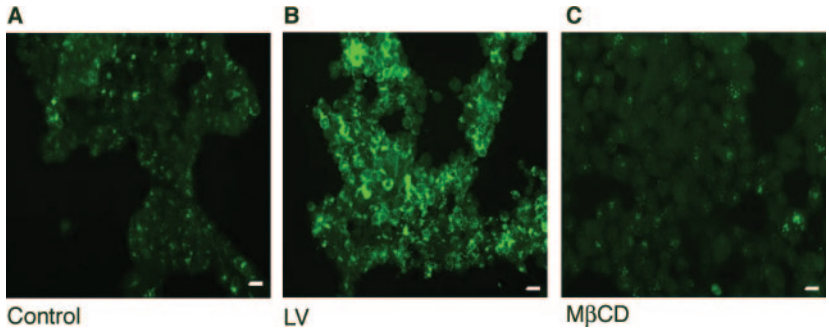

FIG. 4. **Statin causes the accumulation of APPsβ within intracellular compartments.** APPsw-293 cells were exposed to vehicle (*Control*), 10 μM LV for 48 h in FBS, or 10 mM MβCD for 30 min. Following treatment, cells were fixed and sequentially incubated with anti-APPsβsw antiserum and fluorescein 5-isothiocyanate-conjugated goat anti-rabbit antibodies to visualize intracellular APPsβsw (*green*). Note the profound accumulation of APPsβ within intracellular compartments in LV-treated APPsw-293 cells. MβCD treatment showed the opposite effect, with reduced intracellular APPsβ immunoreactivities compared with the control. *Scale bars* = 10 μm.

~400% of control values for the 10 μM doses (Fig. 5*C*).

Taken together, our results thus far demonstrated that statin treatments induced the accumulation of APP, C99, APPsβ, and Aβ40 within cells in a dose-dependent manner. The cell-associated increases in these species occurred regardless of whether cells were treated in medium containing FBS (Condition 1, normal cholesterol and low isoprenoid levels) or LDFBS (Condition 2, low cholesterol and low isoprenoid levels). In addition, C83 levels increased markedly following statin treatment of LDFBS-maintained cells and were inversely correlated with cellular cholesterol levels. However, most importantly, our data suggest that low cellular isoprenoid levels may be responsible for increased β-secretase cleavage and intracellular accumulation of C99, APPsβ, and Aβ and that cellular cholesterol levels may not play a significant role in mediating these effects.

Mevalonate Supplementation Rescues Statin-induced Accumulation of Cell-associated Amyloidogenic Fragments by Providing for GGPP Biosynthesis—Previous studies have demonstrated that supplementation of statin-treated cells with 0.25 mM mevalonate rescues isoprenoid production without significantly increasing cholesterol biosynthesis (34, 37, 38, 52, 54–56). Therefore, to investigate the role of the isoprenoids in the statin-induced buildup of APP, C99, APPsβ, and Aβ40 within cells, we treated APPsw-293 cells with different concentrations of LV in the presence of 0.25 mM mevalonate in FBS (Condition 3, normal cholesterol and normal isoprenoid levels) or LDFBS (Condition 4, low cholesterol and normal isoprenoid levels). We then harvested cell lysates for immunoblot analysis and Aβ ELISAs as described above and compared the results with those obtained for LV-treated cells in FBS (Condition 1, normal cholesterol and low isoprenoid levels) or LDFBS (Condition 2, low cholesterol and low isoprenoid levels). Application of 0.25 mM mevalonate alone to either FBS- or LDFBS-maintained cells had no apparent effect on the levels of cell-associated and secreted APP or APP-derived fragments (data not shown).

Supplementation of LV-treated cells with 0.25 mM mevalonate in FBS-containing medium completely prevented the statin-induced increases in the levels of cell-associated FL-APP, APPsβ, and C99 and the other APP-derived fragments that were observed following treatment with LV alone (Fig. 3, compare *A* with *B*; *G* and *H*). In addition, cell-associated Aβ40 levels in statin-treated cells were reduced to control values by mevalonate supplementation (Fig. 5, *A–C*). This rescue of statin-induced increases by 0.25 mM mevalonate under normal cholesterol conditions (FBS) provides further evidence that isoprenoids affect intracellular levels of β-secretase-cleaved APP fragments and Aβ in a cholesterol-independent manner.

Next, we wanted to determine the effects of mevalonate supplementation on statin-treated cells in a low cholesterol environment (LDFBS). Similar to the results observed with FBS plus mevalonate, 0.25 mM mevalonate in LDFBS-containing medium greatly inhibited statin-induced increases in the levels of C99 and cell-associated APPsβ (Fig. 3, compare *D* and *E*; *H*). Moreover, intracellular Aβ40 levels were equivalent to vehicle control levels following mevalonate supplementation in LDFBS (Fig. 5, *A–C*). These results again indicate that low cellular isoprenoid levels promote β-secretase cleavage and the intracellular accumulation of Aβ and β-secretase-cleaved fragments, whereas cellular cholesterol levels do not appear to play a predominant role.

In contrast to mevalonate supplementation in FBS, LDFBS plus 0.25 mM mevalonate did not completely block the statin-induced accumulation of FL-APP as determined by immunoblot analysis with anti-FL-APP antibodies (Fig. 3, *E* and *G*). Mevalonate supplementation in LDFBS did, however, blunt the FL-APP increase at the lower LV doses (Fig. 3, compare *D* and *E*; *G*). The failure of mevalonate supplementation to completely rescue the statin-induced buildup of FL-APP in LDFBS (low cholesterol and normal isoprenoid levels) (Fig. 3*E*) suggests that the increase in cell-associated APP may be partly due to low cellular cholesterol levels because FBS plus 0.25 mM mevalonate (normal cholesterol and normal isoprenoid levels) (Fig. 3*B*) prevented the FL-APP increase. However, isoprenoids must also influence FL-APP levels because statin-induced APP accumulation occurred in FBS (normal cholesterol and low isoprenoid levels) (Fig. 3*A*), although it was blunted at low LV concentrations (Fig. 3*G*). Thus, FL-APP levels in the cell appear to be affected by both cholesterol-dependent and isoprenoid-dependent mechanisms.

We also observed that C83 levels did not substantially change in cells treated with LV in LDFBS plus 0.25 mM mevalonate (Fig. 3*E*) compared with cells exposed to LV alone in LDFBS (Fig. 3*D*). In contrast, as already noted, C99 levels were dramatically reduced by addition of mevalonate. Because cells grown in statin plus LDFBS-containing medium had low cellular cholesterol levels regardless of mevalonate supplementation, but varied with respect to their isoprenoid levels, a low cholesterol environment appears to favor α-secretase processing of APP, whereas isoprenoids may have less influence on non-amyloidogenic cleavage.

Mevalonate is an upstream precursor of cholesterol and the nonsterol isoprenoids FPP and GGPP (Fig. 1*A*). Importantly, many cholesterol-independent statin effects may be caused by reduced levels of GGPP (reviewed in Ref. 31). To specifically determine the role of GGPP in the isoprenoid-dependent accumulation of FL-APP, APPsβ, C83, and C99 in the absence of changes in total cholesterol, we supplemented LV-treated cells with 10 μM GGPP in FBS (normal cholesterol and normal GGPP levels) (Fig. 3*C*) and compared the effects on APP metabolism with those obtained following LV treatment alone in

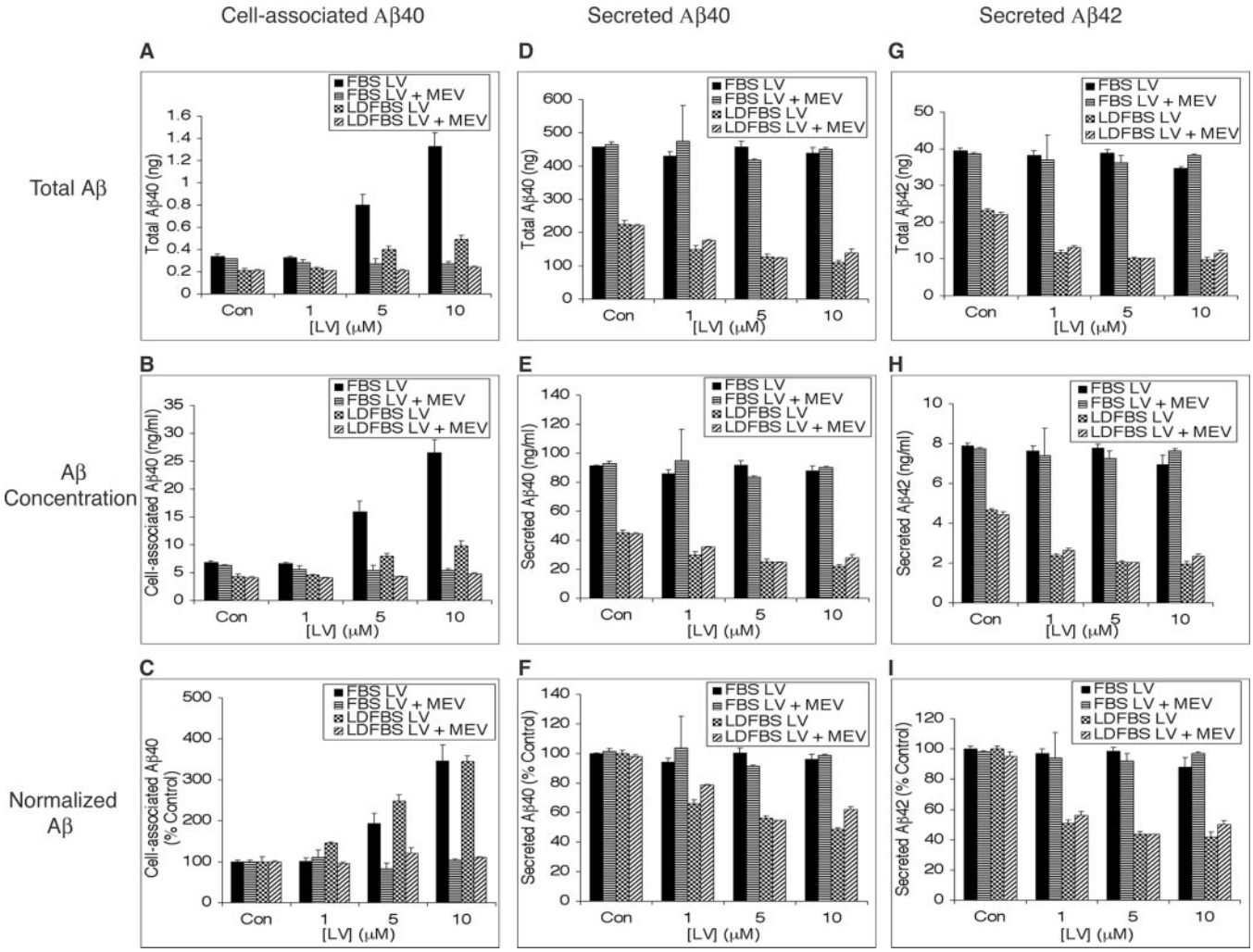

FIG. 5. **Differential isoprenoid-dependent and cholesterol-dependent effects on cell-associated and secreted Aβ, respectively.** APPsw-293 cells were treated for 48 h with vehicle (control (*Con*)) or the indicated concentrations of LV in the absence or presence of 0.25 mM mevalonate (*MEV*) in either FBS- or LDFBS-containing medium. *A–C*, following extraction of Aβ from cells with guanidine HCl, cell-associated Aβ40 levels were measured by specific sandwich ELISAs. *A*, total cell-associated Aβ40 (nanograms ± S.E.); *B*, average Aβ40 concentration within the cell (nanograms/ml ± S.E.); *C*, cell-associated Aβ40 normalized to protein content (percent of the control ± S.E.). LV treatment induced a dose-dependent increase in cell-associated Aβ40 levels in both FBS- and LDFBS-maintained cells, indicating that the effect was cholesterol-independent. Mevalonate supplementation prevented the intracellular Aβ40 increase, demonstrating that it was dependent upon isoprenoids. Cell-associated Aβ42 levels were below the detection limit of the ELISA. *D–I*, the media from treated APPsw-293 cells were collected and assayed by ELISA for Aβ40. *D*, total secreted Aβ40 (nanograms ± S.E.); *E*, Aβ40 concentration in the media (nanograms/ml ± S.E.); *F*, secreted Aβ40 (percent of the control ± S.E.); *G*, total secreted Aβ42 (nanograms ± S.E.); *H*, Aβ42 concentration in the media (nanograms/ml ± S.E.); *I*, secreted Aβ42 (percent control ± S.E.). Although the Aβ40 and Aβ42 levels in the media were at control values for LV-treated cells in FBS (with and without mevalonate), the secreted Aβ40 and Aβ42 levels were only ~50% of control levels for LV-treated cells in LDFBS (with and without mevalonate) (*e.g. F* and *I*), indicating that the reduced Aβ secretion was due to an effect of cholesterol and was independent of isoprenoids.

FBS (Fig. 3*A*). Similar to the results observed with mevalonate supplementation (Fig. 3*B*), 10 μM GGPP completely prevented the statin-induced increases in the levels of cell-associated FL-APP, APPsβ, and C99 and the other APP-derived fragments (Fig. 3, compare *C* with *A*). These results demonstrate that low levels of the isoprenoid GGPP are the major cause of the cell-associated accumulation of amyloidogenic fragments during statin treatment.

In summary, our results with mevalonate supplementation further support the view that low cellular isoprenoid levels enhance β-secretase cleavage and the accumulation of intracellular Aβ and β-secretase-cleaved APP fragments. Furthermore, using GGPP supplementation, we have conclusively demonstrated that the statin-induced accumulation of amyloidogenic fragments is specifically due to the suppression of GGPP biosynthesis. Conversely, low cellular cholesterol levels increase processing in the non-amyloidogenic α-secretase pathway. Finally, both low cholesterol and low isoprenoid levels appear to act additively to increase FL-APP levels in cells.

Low Cellular Cholesterol Levels Enhance and Suppress the α- and β-Secretase Pathways, Respectively—Our work thus far focused on the effects of cholesterol and isoprenoids on cell-associated APP fragments and Aβ, but we were also interested in determining how statin treatments in our system affect secreted APP products, *i.e.* APPsα, APPsβ, and Aβ. Therefore, we treated APPsw-293 cells with LV in FBS or LDFBS with or without 0.25 mM mevalonate and analyzed the conditioned media for APPsα and APPsβ by immunoblotting and for Aβ40 and Aβ42 by specific ELISAs. To detect APPsα, we incubated immunoblots with antibody 6E10, which recognizes Aβ-(1–17), which is present at the C terminus of APPsα. In FBS-containing medium, neither APPsα nor APPsβ levels changed significantly following exposure to statin compared with the vehicle control levels (Fig. 6, *A* and *E*). On the other hand, the medium from LV-treated cells grown in LDFBS showed a

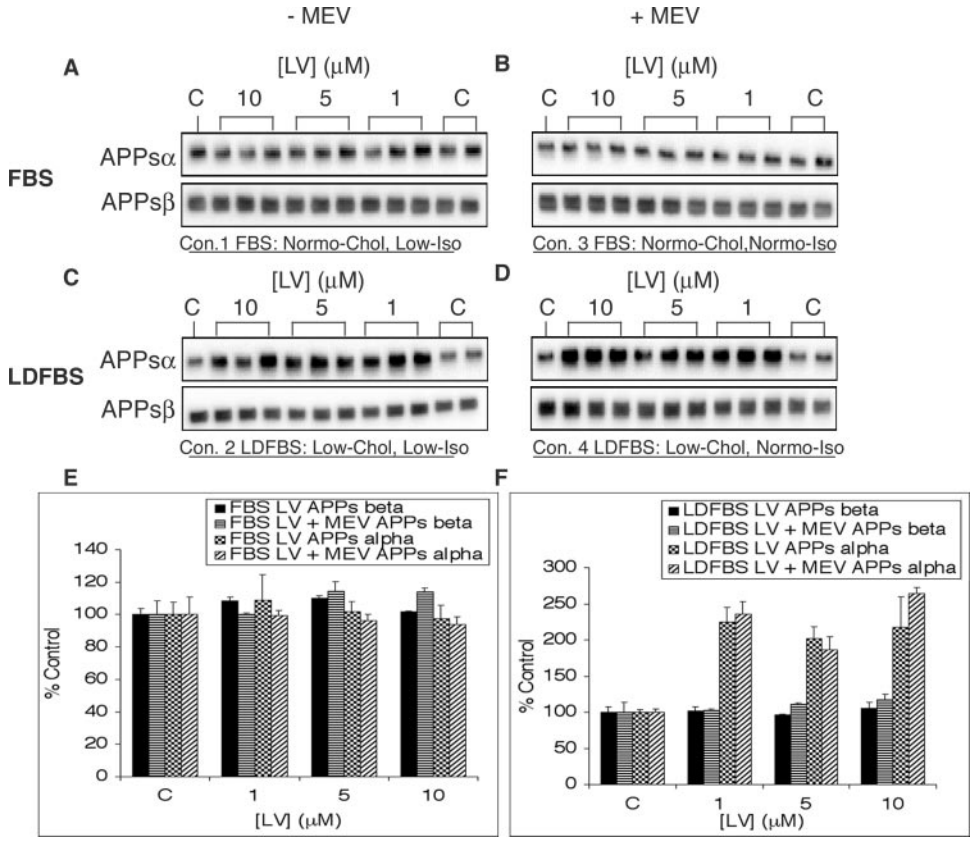

FIG. 6. **Statin increases APPsα secretion in a manner fully dependent on cholesterol reduction.** APPsw-293 cells were treated with vehicle (control (*C*)) or the indicated concentrations of LV for 48 h in FBS (*A*, *B*, and *E*) or LDFBS (*C*, *D*, and *F*) and in the absence (*A* and *C*) or presence (*B* and *D*) of 0.25 mM mevalonate (*MEV*). Following treatment, the media were collected and analyzed by immunoblotting to identify APPsα (antibody 6E10) (*upper panels*) and APPsβ (anti-APPsβsw antiserum) (*lower panels*). *Con.*, conditions described under "Results"; *Normo*, normal; *Chol*, cholesterol; *Iso*, isoprenoids. The immunoblots in *A–D* were scanned on a PhosphorImager; signals were quantified and normalized against total protein concentration; and values are presented as a percentage of the control ± S.E. (*E* and *F*). Note that APPsα levels in the media were increased only in LDFBS (low cellular cholesterol conditions) (*C*, *D*, and *F*) and were not influenced by isoprenoid levels. Secreted APPsβ levels did not appear to change relative to the control under any conditions.

consistent ~2-fold increase in APPsα levels, but APPsβ levels remained at control values (Fig. 6, *C* and *F*). Like the increase in C83 levels observed for LV-treated cells in LDFBS (Fig. 3, *D* and *E*), the levels of APPsα in conditioned medium reached maximum values at the lowest LV dose tested (1 μM) (Fig. 6*F*). Mevalonate supplementation did not significantly alter the levels of either APPsα or APPsβ in conditioned medium compared with mevalonate-minus medium (Fig. 6, compare *A* with *B* and *C* with *D*). These results clearly show that the increase in APPsα levels in the medium is associated with low cellular cholesterol levels (because it occurred exclusively in LDFBS) and is unrelated to isoprenoid levels (because mevalonate supplementation had no effect). The lack of any change in APPsβ secretion into the medium, regardless of isoprenoid status, was unexpected given the strong statin-induced increase in intracellular APPsβ with low isoprenoid levels (Fig. 3, *A*, *D*, and *F*).

Because a low cholesterol environment appears to enhance the non-amyloidogenic α-secretase pathway, Aβ secretion should decrease under conditions that lower total cellular cholesterol levels in our system. To test this hypothesis, we measured Aβ40 and Aβ42 in the conditioned medium from the same LV-treated APPsw-293 cells that were analyzed for secreted APPsα and APPsβ. As reported previously, the total amount of secreted Aβ40 was ~10-fold higher than the total amount of secreted Aβ42 in all samples (~400 and ~40 ng, respectively) (Fig. 5, *D* and *G*). In addition, the levels of secreted Aβ40 and Aβ42 were significantly reduced in untreated cells maintained in LDFBS compared with cells maintained in FBS (Fig. 5, *D*, *E*, *G*, and *H*). The reduction of secreted Aβ levels in LDFBS was not due to decreased FL-APP levels because vehicle control APPsw-293 cells had similar levels of FL-APP in both LDFBS and FBS as determined by antibody 22C11 immunoblot analysis (Fig. 3*J*). Most importantly, we observed that the levels of both secreted Aβ40 and Aβ42 were reduced to ~50% of control values following treatment with LV in LDFBS either with or without mevalonate supplementation (Fig. 5, *D–I*). In contrast, secreted Aβ40 and Aβ42 levels from LV-treated cells in FBS were not significantly different from control levels. Thus, the decrease in the levels of Aβ40 and Aβ42 secreted into the medium was strongly associated with low cellular cholesterol levels (Conditions 2 and 4) and did not correlate with isoprenoid status in cells. In this regard, secreted Aβ40 and Aβ42 on the one hand and secreted APPsα on the other exhibited cholesterol-dependent and isoprenoid-independent behaviors, although the respective levels of secreted Aβ and APPsα changed in opposite directions following treatment.

To confirm by another method that low cellular cholesterol levels enhance the α-secretase pathway and thereby indirectly suppress β-secretase processing, we treated APPsw-293 cells with 10 mM MβCD and performed immunoblot analysis on cell lysates for C83 and APPsβ. Unlike statin treatment, which inhibits *de novo* cholesterol synthesis in the ER, MβCD preferentially removes cholesterol from the plasma membrane (34, 37, 57). As observed for statin-treated cells maintained in LDFBS (Fig. 3, *D* and *E*), exposure to MβCD resulted in an increase in C83 levels (Fig. 7*A*). However, in contrast to statin treatment, MβCD reduced the level of cell-associated APPsβ to

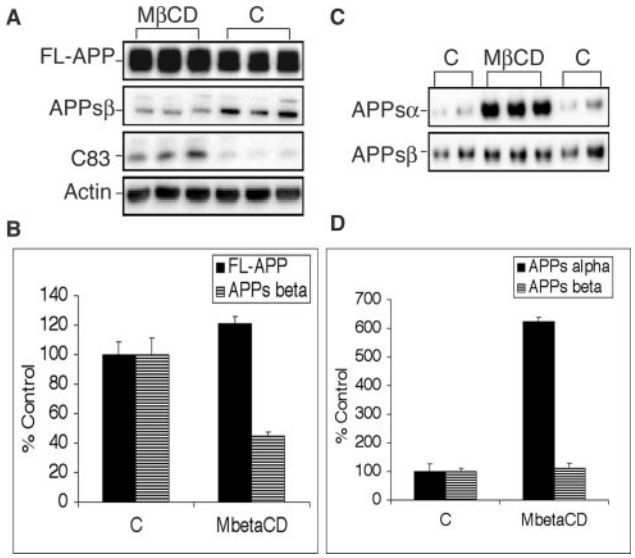

FIG. 7. **Reduced cellular cholesterol favors α-secretase over β-secretase processing of APP.** APPsw-293 cells were treated with vehicle (control (*C*)) or 10 mM MβCD for 30 min in FBS-containing medium, and then cell lysates (*A* and *B*) and media (*C* and *D*) were harvested and analyzed by immunoblotting with anti-APP-(676–695) antiserum (FL-APP and C83), anti-APPsβsw antiserum (APPsβ), antibody 6E10 (APPsα), and anti-actin antibody (loading control). The immunoblots were scanned on a PhosphorImager, quantified, and normalized against actin signal (cell lysates) or total cellular protein concentration (media) and are expressed as a percentage of the control ± S.E. (*B* and *D*). Note that lowering the total cellular cholesterol levels with MβCD (*MbetaCD*) caused an increase in the levels of α-secretase cleavage products C83 (*A*) and APPsα (*C*) and a decrease in the levels of intracellular APPsβ (*A* and *B*). A slight increase in FL-APP levels was also observed following MβCD treatment (*A* and *B*). Similar effects were observed for cells maintained and treated in LDFBS (not shown).

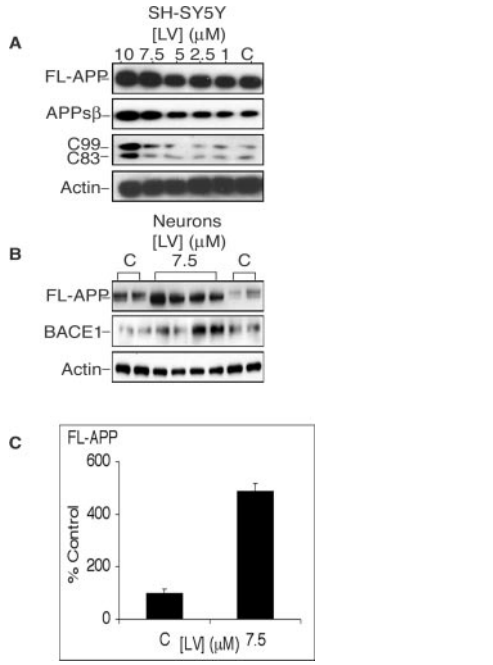

FIG. 8. **Statin induces the accumulation of cell-associated APP and APP fragments in neural cells.** Human SH-SY5Y neuroblastoma cells (*A*) and mouse Tg2576 primary cortical neurons (*B* and *C*) were treated with vehicle (control (*C*)) or the indicated concentrations of LV for 48 h. Prior to LV exposure, SH-SY5Y cells were infected with APPsw adenovirus for 48 h. Following LV treatment, cell lysates were prepared and analyzed by immunoblotting with anti-APP-(676–695) antiserum (FL-APP, C99, and C83), anti-APPsβsw antiserum, anti-BACE1 antibody, and anti-actin antibody. Cell-associated FL-APP levels and cleaved APP fragments were increased in SH-SY5Y cells by LV (*A*). For primary neurons, FL-APP immunoblot signals were scanned on a PhosphorImager, quantified, and normalized against actin and are presented as a percentage of the control ± S.E. (*C*). Note that LV treatment increased the levels of both FL-APP and BACE1 in primary neurons (*B*).

~40% of control values (Fig. 7, *A* and *B*) and visibly decreased intracellular APPsβ accumulation as determined by anti-APPsβsw immunofluorescence microscopy (Fig. 4*C*). The levels of FL-APP appeared slightly increased by MβCD treatment in our system (Fig. 7, *A* and *B*), in agreement with our previous conclusion that low cellular cholesterol contributes to elevated FL-APP levels (Fig. 3*E*).

Next, we measured APPsα and APPsβ levels in the conditioned medium from MβCD-treated cells. Similar to the effects of statin treatment in LDFBS-containing medium (Fig. 6, *C* and *D*), we observed an elevation of APPsα levels in the medium compared with control levels and detected no change in APPsβ levels (Fig. 7, *C* and *D*). The increase in secreted APPsα mirrored the rise in C83 levels observed following exposure to MβCD (Fig. 7*A*). It is notable that the magnitude of the APPsα increase was large (~600% of control values) and exceeded that observed for LV-treated cells in LDFBS (Fig. 6, *C*, *D*, and *F*). The more robust APPsα secretion may be related to the greater ability of MβCD to lower total cellular cholesterol levels compared with statin treatment in LDFBS (Fig. 2). In any case, taken together, our results with both LV treatment in LDFBS and MβCD treatment demonstrate that low cellular cholesterol levels enhance α-secretase processing of APP, as indicated by higher levels of C83 and secreted APPsα, and suppress the β-secretase pathway, as shown by lower levels of intracellular APPsβ (MβCD) (Fig. 7*A*) and secreted Aβ (LV in LDFBS) (Fig. 5, *D–I*).

Statins Induce the Accumulation of Cell-associated β-Secretase-cleaved APP Fragments in Neural and Astrocyte Cells—Although HEK293 cells have been widely used to study APP processing, they are not of central nervous system origin and therefore may not exhibit the same statin-induced effects as those of physiologically relevant cell types involved in AD. To address this concern, we statin-treated several neural and astrocyte cell types, such as human SH-SY5Y neuroblastoma cells and mouse primary cortical neurons and astrocytes, and performed immunoblot analysis on cell lysates for FL-APP, C83, C99, APPsβ, and the β-secretase enzyme BACE1. Prior to treatment, SH-SY5Y cells were infected for 2 days with adenovirus carrying a transgene that induces high level expression of human APP695sw. Cells were then treated with different concentrations of LV for 48 h, and cell lysates were prepared for immunoblot analysis using anti-APP-(676–695) and anti-APPsβsw antisera. We observed dose-dependent increases in FL-APP and the β-secretase-cleaved APPsβ and C99 fragments in LV-treated SH-SY5Y cells (Fig. 8*A*), similar to statin-treated APPsw-293 cells. C83 levels also rose somewhat upon statin treatment, but appeared less dramatic compared with the C99 increase.

Next, we cultured primary cortical neurons isolated from transgenic mice expressing APP695sw (Tg2576) (61) and treated them with 7.5 μM LV for 48 h. The purity of our neuronal cell cultures was >95% as determined by β-tubulin III immunofluorescence microscopy (data not shown). Immunoblot analysis of lysates from LV-treated Tg2576 neurons using anti-APP-(676–695) antiserum revealed that FL-APP levels were increased to ~500% of control Tg2576 neuron values (Fig. 8, *B* and *C*), which is similar in magnitude to the APP increases observed in statin-treated APPsw-293 cells (Fig. 3*G*).

It is interesting to note that, in most cell types we analyzed, statin treatment appeared to elevate the level of C99 to a

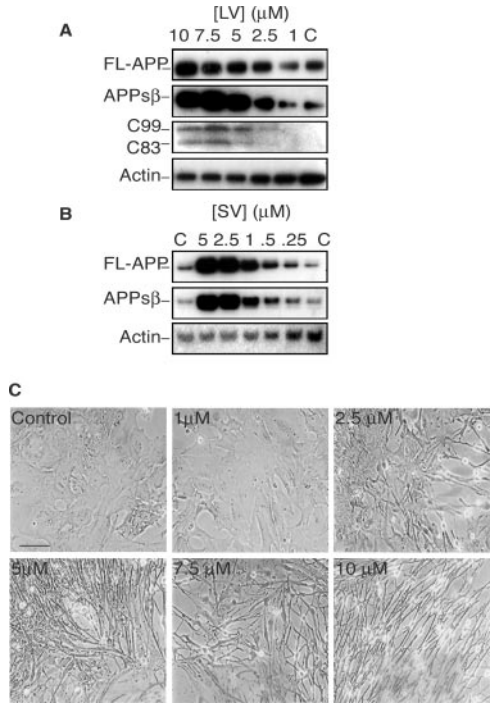

FIG. 9. **Statins induce the accumulation of cell-associated APP and APP fragments in astrocytes and appear to cause morphological activation.** Tg2576 astrocytes were treated with vehicle (control (*C*)) or the indicated concentrations of LV (*A* and *C*) or SV (*B*) in FBS-containing medium for either 48 h (*A* and *C*) or 96 h (*B*). Cell lysates were then harvested for immunoblot analysis (*A* and *B*), or astrocytes were micrographed (*C*). Anti-APP-(676–695) antiserum (FL-APP, C83, and C99), anti-APPsβsw antiserum, and anti-actin antibody were used for immunoblot analysis. LV and SV caused a dose-dependent elevation of cell-associated APP and APP fragments, and increases were detected even at the lowest dose (0.25 μM SV) (*B*). Similar changes were observed in astrocytes maintained in LDFBS-containing medium (not shown). Astrocytes appeared to take on an activated morphology with increasing LV doses (*C*), paralleling the rising levels of APP and cleaved APP fragments. *Scale bar* = 100 μm.

greater extent than that of C83 (*e.g.* Fig. 3). Intriguingly, the level of the β-secretase enzyme BACE1 was increased in LV-treated neurons compared with controls (Fig. 8*B*), suggesting the possibility that higher BACE1 levels may be responsible for the enhanced production of C99 (and APPsβ) over that of C83 in treated cells. Further investigation will be required to determine the potential role of elevated BACE1 levels in driving the statin-induced increases in C99.

In another series of experiments, we treated purified cultures of astrocytes isolated from Tg2576 mice with different concentrations of LV and SV and then analyzed cell lysates for APP and cell-associated APP-derived fragments by immunoblotting. As with APPsw-293 cells and neural cell types, statin treatment resulted in significant dose-dependent increases in the levels of FL-APP and β-secretase-cleaved C99 and APPsβ within astrocytes (Fig. 9, *A* and *B*). Statins also appeared to raise C83 levels somewhat, but to a lesser extent than C99 levels. In addition, we noticed that the morphology of statin-treated astrocytes changed dramatically from a flat cobblestone appearance (control) to a shape with elongated processes resembling an activated phenotype (Fig. 9*C*). Previous studies have shown that statins can alter cell morphology by inhibiting isoprenylation of proteins that affect cytoskeletal structure and dynamics (*e.g.* RhoA and Rac) (32, 33), so it is tempting to speculate that the statin-induced changes in astrocyte shape may be due to an isoprenoid-dependent mechanism.

It has been reported that statins exhibit pleiotropic effects (30, 31), and although previous studies have typically used high doses of statins, it was conceivable that our results may have been an artifact of the relatively high concentrations of LV and SV used in our study. To exclude this possibility, we treated several different cell types with lower concentrations of LV and SV and performed immunoblot analysis on cell lysates for APP and APP-derived fragments. In one representative experiment, we cultured Tg2576 astrocytes with a range of SV concentrations from 0.25 to 5 μM for 96 h, and we observed significant accumulation of FL-APP and APPsβ within astrocytes even at the lowest SV concentration (Fig. 9*B*). These data show that cell-associated accumulation of APP and APP-derived fragments is not an artifact of high statin concentration. Moreover, taken together, our results with APPsw-293, neural, and astrocyte cells demonstrate that statins induce the accumulation of APP and cell-associated β-secretase-cleaved APP fragments in a variety of cell types, including those of relevance to AD.

DISCUSSION

Model for Isoprenoid-dependent and Cholesterol-dependent Effects on APP Processing—Our analysis of cholesterol-dependent *versus* isoprenoid-dependent effects of statins on APP processing allowed us to make the following conclusions. (i) We report for the first time that low cellular isoprenoid levels cause the intracellular accumulation of full-length APP and the β-secretase-cleaved fragments APPsβ, C99, and, most significantly, Aβ. (ii) In contrast, low cellular cholesterol levels elevate α-secretase cleavage of APP and consequently reduce Aβ secretion, as reported previously (34, 37, 38) (iii) Importantly, these cholesterol and isoprenoid effects behave independently of one another, suggesting that they work through unrelated mechanisms.

The major focus of this study was the development of an effective *in vitro* system that would enable the discrete analysis of specific statin effects on APP metabolism, and to this end, a robust non-neuronal HEK293 cell type was employed. In addition, we examined statin effects on APP metabolism in AD-relevant neural cell types. Importantly, statins elevated intracellular levels of APP and β-secretase-cleaved fragments in all cell types analyzed. These effects were not due to statin-induced increases in APP transgene expression or mRNA stability. Moreover, the accumulation of cell-associated FL-APP and β-secretase-cleaved fragments occurred even at low, physiologically relevant (nanomolar) statin concentrations and thus was not an artifact of high drug doses.

Our results are consistent with a model in which low cellular isoprenoid levels inhibit the trafficking of APP through the secretory pathway. Assuming that the rates of APP protein synthesis and degradation remain unchanged, reduced transport of APP through the secretory pathway would lead to elevated levels of APP in biosynthetic compartments (*i.e.* ER, Golgi, and *trans*-Golgi network (TGN)) (Fig. 10). This would account for our observation that immature APP levels were increased upon statin inhibition of isoprenoid synthesis (Fig. 3, *A*, *D*, *F*, and *I*). Because the TGN is a major site of BACE1 intracellular localization (18), accumulation of APP in the TGN would raise rates of enzyme-substrate interaction and subsequent β-secretase cleavage of APP, thus increasing APPsβ and C99 levels. This effect could be exacerbated by concomitant accumulation of BACE1, as suggested by our data in primary neurons (Fig. 8*B*). Finally, γ-secretase is also localized within the TGN (62), leading to increased conversion of C99 into Aβ and accumulation of intracellular Aβ.

In contrast, low cellular cholesterol levels do not appear to significantly inhibit outward transport of APP, but may instead reduce the rate of endocytosis of cell-surface APP, as suggested previously (38, 57). Thus, cell-surface APP levels would become elevated, and the rate of APP processing by α-secretase, which

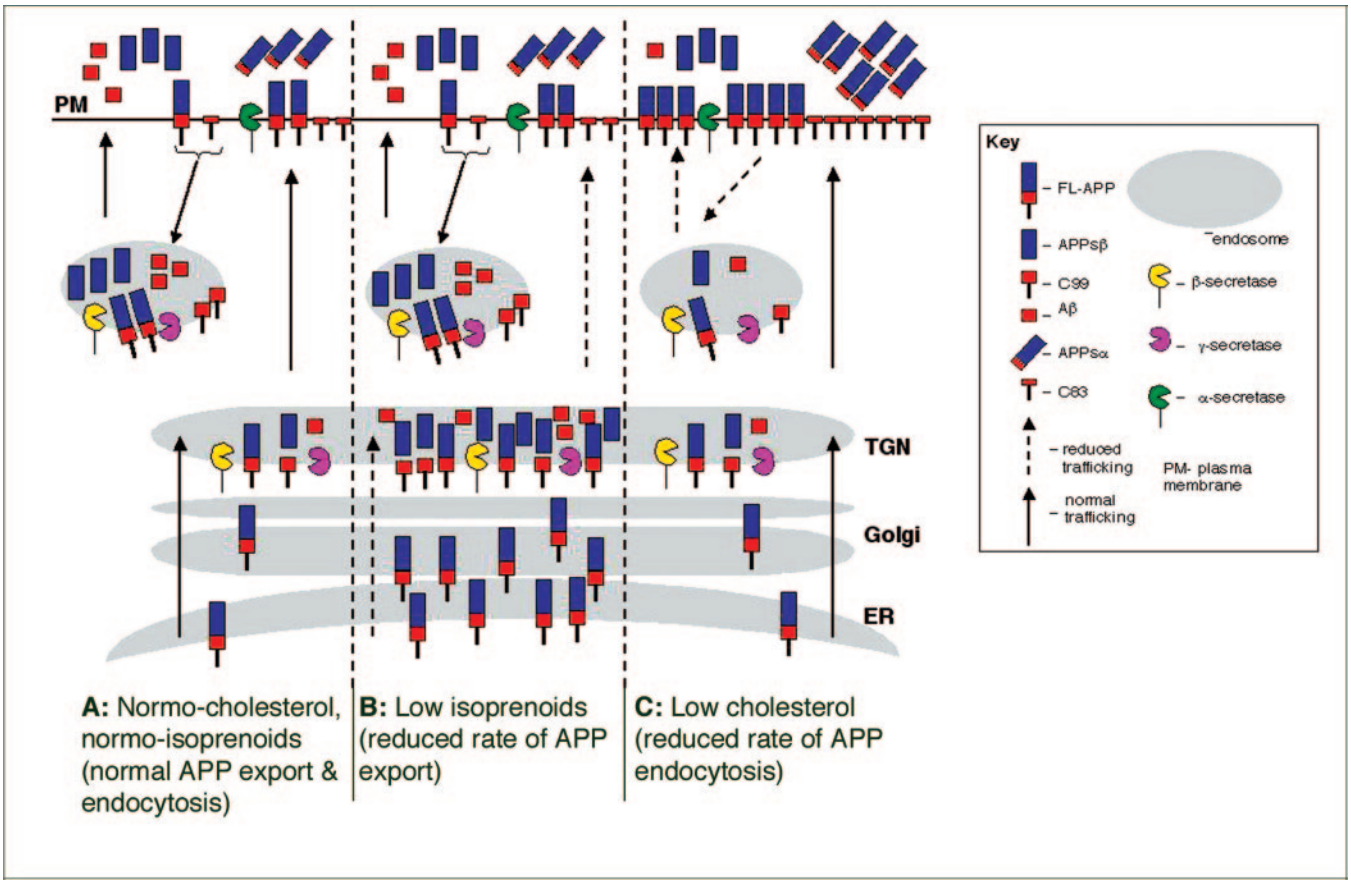

FIG. 10. **Model for low isoprenoid *versus* low cholesterol effects on APP processing in cells.** Under conditions of normal (*Normo*) cholesterol and isoprenoid levels (*A*), the rate of APP export through the secretory pathway to the plasma membrane (*PM*) is rapid, as are the rates of endocytosis and trafficking of APP to the endosome, where the majority of β-secretase processing normally occurs. APP at the plasma membrane may also be cleaved by α-secretase before being endocytosed. Importantly, two independent pools of Aβ are generated, one made in the TGN and the other produced in the endosome. When isoprenoid levels are low (*B*), the rate of APP export is reduced, and APP accumulates in the biosynthetic compartments of the secretory pathway. Because the TGN is a site of β- and γ-secretase localization, β-secretase-cleaved fragments and Aβ accumulate within this intracellular compartment. In contrast, the endosomal pathway of Aβ generation appears unaffected by low isoprenoid levels, as is α-secretase processing of APP at the plasma membrane. Under low cellular cholesterol conditions (*C*), APP export through the secretory pathway is normal; however, the rate of APP endocytosis to the endosome is reduced. Consequently, APP levels at the plasma membrane are increased, thus allowing greater α-secretase cleavage of APP. As a result of reduced APP endocytosis and increased α-secretase processing, less APP is cleaved by β-secretase in the endosome; hence, the endosomal pool of Aβ is reduced.

resides on the plasma membrane, would increase. This hypothesis is supported by the increased levels of C83 and APPsα that we (Fig. 7, *A*, *C*, and *D*), and others (37, 38) have observed under low cellular cholesterol conditions. Moreover, a cholesterol-dependent decrease in the rate of APP endocytosis would reduce the levels of APP in endosomal compartments, also sites of BACE1 and γ-secretase localization, and would thus lead to lower levels of Aβ production and secretion, as this study and others have shown (34, 37, 38).

Independent Intracellular and Secreted Pools of Aβ—We have provided evidence for two cellular pools of Aβ (one intracellular and the other secreted) that behave independently of one another. For example, statin-treated cells in FBS (Condition 1, normal cholesterol and low isoprenoid levels) or LDFBS (Condition 2, low cholesterol and low isoprenoid levels) both accumulated intracellular Aβ to levels that were ~4-fold above control values, yet Condition 1 cells secreted control levels of Aβ, whereas Condition 2 cells secreted only about half that amount (Fig. 5). Conversely, cells grown in LDFBS plus mevalonate (Condition 4, low cholesterol and normal isoprenoid levels) had control levels of intracellular Aβ (unlike Condition 2 cells) and secreted low levels of Aβ (similar to Condition 2 cells). Thus, the intracellular Aβ pool is affected by isoprenoids, whereas the secreted Aβ pool is influenced by cholesterol.

We noted that the amount of total intracellular Aβ40 was small compared with that of total extracellular Aβ40 (*e.g.* ~0.45% for 10 μM statin-treated LDFBS cells) (Fig. 5, *A* and *D*). However, comparisons of total Aβ levels in the medium *versus* cell lysates are not true indications of the relative rates of Aβ production in the two compartments because the respective rates of Aβ degradation in the medium *versus* the cell are unknown and may differ widely. In fact, it is possible that the production rates of secreted and intracellular Aβ may be similar, but Aβ degradation may be more rapid within the cell than in the medium, leading to the accumulation of greater absolute amounts of secreted Aβ compared with intracellular Aβ. Therefore, comparisons of total Aβ amounts have the potential to be misleading and may lead to the false impression that cell-associated Aβ production is not significant. Indeed, our estimate of Aβ40 concentrations within the cell (total cell-associated Aβ40 divided by the cell pellet volume) (Fig. 5*B*) is significant (*e.g.* ~45% of the media Aβ40 concentration for 10 μM statin-treated LDFBS cells) (Fig. 5*E*). Moreover, we predict much higher Aβ concentrations within the intracellular compartments in which Aβ accumulation occurs. The major findings of this study are that intracellular Aβ levels increase dramatically upon statin-induced inhibition of isoprenoid synthesis and that distinct pools of intracellular and secreted Aβ exist that are largely isoprenoid-dependent and cholesterol-dependent, respectively. Although the consequences of high in-

tracellular Aβ concentrations are not fully understood, mounting evidence suggests that accumulation of intraneuronal Aβ may play an early role in AD pathogenesis (5–15). Thus, we suggest that the isoprenoid-dependent accumulation of cell-associated Aβ represents a significant finding that may have important implications for mechanisms of AD.

It should be noted that we cannot currently completely exclude the possibility that low isoprenoid levels cause a shift from Aβ secretion to intracellular accumulation. However, because low isoprenoids do not lead to decreases in the levels of secreted Aβ or APPsβ (which is assumed to parallel Aβ), then a shift from secretion to accumulation would have to be relatively small and not result in any detectable reductions in secreted Aβ or APPsβ. We suggest that this scenario is unlikely because the dramatic isoprenoid-dependent increase in the levels of cell-associated Aβ and APPsβ that we observed would be expected to be associated with decreases in secreted Aβ and APPsβ levels if a significant shift from secretion to accumulation had occurred. Instead, our results support the hypothesis that low isoprenoid levels promote the accumulation of an intracellular Aβ pool without significantly affecting the secreted Aβ pool and are consistent with previous studies demonstrating an intracellular Aβ pool (63). To our knowledge, this study is the first to show that the distinct intracellular and secreted Aβ pools are differentially affected by cellular isoprenoid and cholesterol levels, respectively.

Isoprenoid-dependent Mechanisms Underlying the Effects of Statins on APP Metabolism—Our model in which low isoprenoid levels slow down APP transport through the secretory pathway is supported by evidence that inhibition of isoprenylation of key regulatory proteins involved in protein trafficking (*e.g.* G-proteins in the Rho and Rab families) is associated with cytoskeletal alterations and a decrease in the efficiency of vesicular transport (64, 65). In this study, statin-induced increases in intracellular APP and its metabolites were prevented by addition of mevalonate in a manner that did not significantly affect total cellular cholesterol levels. As detailed above, mevalonate is required for the biosynthesis of FPP and GGPP as well as cholesterol. GGPP predominantly functions to isoprenylate (geranylgeranylate) a large number of target proteins, whereas the number of farnesylated proteins is less (66–68). Furthermore, FPP is generally accepted to be the common branch point in the cholesterol pathway, being a metabolic precursor of both sterol (*e.g.* cholesterol) and nonsterol (*e.g.* GGPP) products. Here, the dependence of APP and amyloidogenic fragment accumulation on inhibition of nonsterol isoprenoid synthesis was established by the demonstration that these effects were fully rescued with GGPP supplementation, further suggesting the involvement of isoprenylated G-proteins. Indeed, previous studies have demonstrated that geranylgeranylated G-proteins such as Rab1B (69) and Rab6 (70) play an important role in the trafficking and processing of APP. Although further investigation is required to determine the identity of the geranylgeranylated target proteins responsible for the effects we have observed, to our knowledge, this study provides the first evidence that interference with isoprenoid synthesis causes the intracellular accumulation of amyloidogenic fragments and Aβ.

As discussed above, the specifics of intracellular APP degradation (and associated fragments) have not been examined in this study. However, in addition to the accumulation of intracellular APP, APPsβ, C99, and Aβ under low isoprenoid conditions, we noted significant buildup of several uncharacterized APP fragments of varying sizes (Fig. 3, *A*, *D*, and *F*). It is possible that these APP fragments are due to a degradation mechanism that rids the cell of excess proteins from intracellular compartments. Further investigation into the nature of these APP fragments is required.

Interestingly, statin treatment under conditions that led to the accumulation of APP and amyloidogenic fragments was dose-dependently coupled to significant alterations in astrocyte morphology, leading to an activated-appearing phenotype. These observations imply a statin-induced rearrangement of the astrocyte cytoskeleton. Recently, Bi *et al.* (32) reported that statins activate microglia through inhibition of isoprenoid biosynthesis. Because G-proteins in the Rho family are involved in regulating the organization of the actin cytoskeleton, it is possible that Rho may play a role in the cytoarchitectural changes that occur upon astrocyte activation. Whether the morphological changes observed in our study are linked to true physiological astrocyte activation remains to be determined.

Cholesterol-dependent Mechanisms Underlying the Effects of Statins on APP Metabolism—As we (this study) and others (34, 37, 57) have shown, total cholesterol levels are reduced by treatment with either statins or MβCD. It is well documented that statins and cyclodextrins lower cellular cholesterol levels via different mechanisms. Statins inhibit cholesterol biosynthesis, whereas MβCD specifically sequesters plasma membrane cholesterol to rapidly depress total cellular cholesterol levels (34, 37, 57). Kojro *et al.* (38) reported previously that more than one mechanism underlies the increase in non-amyloidogenic α-secretase processing of APP following reduction of cellular cholesterol. They showed that impaired internalization of APP and increased membrane fluidity are responsible for increased α-secretase cleavage after acute cholesterol depletion by MβCD, whereas LV stimulates APPsα secretion by increasing the expression of ADAM10 (a disintegrin and metalloprotease). Although we did not analyze the specific mechanisms by which MβCD and statins increase the non-amyloidogenic processing of APP, it is possible that the observed statin-induced cholesterol-dependent increases in α-secretase processing might be due in part to elevated ADAM10 levels or activity. In addition, the mechanistic differences in the cholesterol-lowering actions of the two drugs may have also contributed to the differential effects on APP processing that we observed.

In our experimental system, although we were able to modulate total cellular cholesterol levels efficiently and thus determine the effects of cholesterol on APP processing, we did not investigate in detail how cholesterol localization within the cell may influence APP cleavage and Aβ production. Cordy *et al.* (71) have demonstrated that localization of BACE1 to cholesterol-rich lipid rafts increases Aβ production and that raft disruption by cholesterol-lowering agents is closely associated with decreased amyloidogenic processing. Their work indicates that Aβ production occurs predominantly in cholesterol-rich rafts and that BACE1 is the rate-limiting enzyme involved in this process. Given these observations, the levels and subcellular distributions of cholesterol and BACE1 in relation to those of APP are expected to play a crucial role in Aβ production.

In this study, filipin staining of cholesterol, followed by immunofluorescence microscopy, did not reveal obvious redistributions of free intracellular cholesterol with any of our treatments (data not shown). However, these were low resolution studies, and we cannot exclude the possibility of subtle changes in cholesterol localization at the subcellular level following statin treatment. Indeed, we speculate that small differences in subcellular cholesterol levels or localization may account for the observation that altering the supply of exogenous cholesterol is associated with changes in total Aβ production. We noted that secreted Aβ levels were significantly lower in untreated cells maintained in LDFBS compared with those maintained in FBS (Fig. 5, *D*, *E*, *G*, and *H*). Although cells main-

tained in either FBS or LDFBS had equivalent total cholesterol levels in the absence of statins (Fig. 2), they differed in how they obtained cholesterol and therefore may have contrasting subcellular cholesterol distributions that could differentially affect Aβ production in secreted and intracellular pools. For cells in LDFBS, cholesterol uptake by receptor-mediated endocytosis is lacking, and we hypothesize that cholesterol levels may consequently be below normal in the plasma membrane and within the endosomal pathway. Because the secreted Aβ pool appears to be generated within the endosomal pathway, low cholesterol levels in this compartment would be expected to reduce the production of secreted Aβ, as is consistent with our results (compare control secreted Aβ levels in FBS *versus* LDFBS) (Fig. 5, *D*, *E*, *G*, and *H*). The intracellular Aβ pool appears to be generated in biosynthetic compartments and thus may be less affected by low cholesterol in the endosomal pathway, which is consistent with our observation that intracellular Aβ levels were only slightly lower in control cells maintained in LDFBS compared with those maintained in FBS (Fig. 5, *A* and *B*). The extent to which cholesterol localization and lipid raft physiology are affected by cholesterol biosynthesis in the ER *versus* cholesterol uptake via receptor-mediated endocytosis remains to be determined.

Finally, other work has demonstrated that aberrant cholesterol trafficking (45) and high cholesterol ester levels (43) are associated with elevated γ-secretase activity and increased Aβ production. Clearly, further investigation into the effects of cholesterol trafficking, localization, and form on APP processing and Aβ generation is warranted.

Conclusion—Although the mechanisms by which statins exert beneficial effects in AD remain unclear, our *in vitro* experiments have established that cellular isoprenoid levels can affect the accumulation of intracellular Aβ and amyloidogenic fragments. Given recent evidence that intracellular Aβ may play a role in AD pathophysiology (5, 6, 8–15), it is critical to investigate the mechanisms of isoprenoid-dependent accumulation of intracellular Aβ and to identify the isoprenylated target proteins that are involved. Such studies may provide useful information for the discovery of novel therapeutic approaches for the treatment of AD.

Acknowledgments—We thank Amgen Inc. for the gift of BACE1$^{-/-}$ mice. We thank the following individuals for input: Erika Maus for maintenance and genotyping of transgenic and knockout mice, Linda Van Eldik, Ling Guo, and Jie Zhao for training and advice on astrocyte culture, Adriana Ferreira for training and advice on primary neuronal culture, Farhad Rahimi-Danesh for helpful discussions, David Dean for the use of his microscope, the staff of the Center for Genetic Medicine (Northwestern University) for the ABI 7900 sequence analyzer, and Steve Adam for training and use of the Kodak Image Analyzer.

Note Added in Proof—While this manuscript was in review, Pedrini *et al.* reported that statins modulate α-secretase processing of APP by ROCK in an isoprenoid-dependent manner (*PLoS Medicine* (2005) **2,** 1–13). In the current study, we did not directly investigate the potential role of ROCK in mediating the effects that we observed, and further research will be required to determine the relationships between our results and those of Pedrini *et al*.

REFERENCES

1. Glenner, G. G., and Wong, C. W. (1984) *Biochem. Biophys. Res. Commun.* **120,** 885–890
2. Masters, C. L., Multhaup, G., Simms, G., Pottigiesser, J., Martins, R. N., and Beyreuther, K. (1985) *EMBO J.* **4,** 2757–2763
3. Younkin, S. G. (1998) *J. Physiol. Paris* **92,** 289–292
4. Selkoe, D. J. (2001) *Physiol. Rev.* **81,** 741–766
5. Gouras, G. K., Tsai, J., Naslund, J., Vincent, B., Edgar, M., Checler, F., Greenfield, J. P., Haroutunian, V., Buxbaum, J. D., Xu, H., Greengard, P., and Relkin, N. R. (2000) *Am. J. Pathol.* **156,** 15–20
6. Blasko, I., Veerhuis, R., Stampfer-Kountchev, M., Saurwein-Teissl, M., Eikelenboom, P., and Grubeck-Loebenstein, B. (2000) *Neurobiol. Dis.* **7,** 682–689
7. Nilsberth, C., Westlind-Danielsson, A., Eckman, C. B., Condron, M. M., Axelman, K., Forsell, C., Stenh, C., Luthman, J., Teplow, D. B., Younkin, S. G., Naslund, J., and Lannfelt, L. (2001) *Nat. Neurosci.* **4,** 887–893
8. Takahashi, R. H., Milner, T. A., Li, F., Nam, E. E., Edgar, M. A., Yamaguchi, H., Beal, M. F., Xu, H., Greengard, P., and Gouras, G. K. (2002) *Am. J. Pathol.* **161,** 1869–1879
9. Takahashi, R. H., Almeida, C. G., Kearney, P. F., Yu, F., Lin, M. T., Milner, T. A., and Gouras, G. K. (2004) *J. Neurosci.* **24,** 3592–3599
10. Gyure, K. A., Durham, R., Stewart, W. F., Smialek, J. E., and Troncoso, J. C. (2001) *Arch. Pathol. Lab. Med.* **125,** 489–492
11. Mori, C., Spooner, E. T., Wisniewsk, K. E., Wisniewski, T. M., Yamaguch, H., Saido, T. C., Tolan, D. R., Selkoe, D. J., and Lemere, C. A. (2002) *Amyloid* **9,** 88–102
12. Busciglio, J., Pelsman, A., Wong, C., Pigino, G., Yuan, M., Mori, H., and Yankner, B. A. (2002) *Neuron* **33,** 677–688
13. Oddo, S., Caccamo, A., Shepherd, J. D., Murphy, M. P., Golde, T. E., Kayed, R., Metherate, R., Mattson, M. P., Akbari, Y., and LaFerla, F. M. (2003) *Neuron* **39,** 409–421
14. Schmitz, C., Rutten, B. P., Pielen, A., Schafer, S., Wirths, O., Tremp, G., Czech, C., Blanchard, V., Multhaup, G., Rezaie, P., Korr, H., Steinbusch, H. W., Pradier, L., and Bayer, T. A. (2004) *Am. J. Pathol.* **164,** 1495–1502
15. Cataldo, A. M., Petanceska, S., Terio, N. B., Peterhoff, C. M., Durham, R., Mercken, M., Mehta, P. D., Buxbaum, J., Haroutunian, V., and Nixon, R. A. (2004) *Neurobiol. Aging* **25,** 1263–1272
16. Vassar, R. (2004) *J. Mol. Neurosci.* **23,** 105–114
17. Sisodia, S. S., Kim, S. H., and Thinakaran, G. (1999) *Am. J. Hum. Genet.* **65,** 7–12
18. Vassar, R., Bennett, B. D., Babu-Khan, S., Kahn, S., Mendiaz, E. A., Denis, P., Teplow, D. B., Ross, S., Amarante, P., Loeloff, R., Luo, Y., Fisher, S., Fuller, J., Edenson, S., Lile, J., Jarosinski, M. A., Biere, A. L., Curran, E., Burgess, T., Louis, J.-C., Collins, F., Treanor, J., Rogers, G., and Citron, M. (1999) *Science* **286,** 735–741
19. Skovronsky, D. M., Moore, D. B., Milla, M. E., Doms, R. W., and Lee, V. M. (2000) *J. Biol. Chem.* **275,** 2568–2575
20. Jarvik, G. P., Wijsman, E. M., Kukull, W. A., Schellenberg, G. D., Yu, C., and Larson, E. B. (1995) *Neurology* **45,** 1092–1096
21. Kivipelto, M., Helkala, E. L., Laakso, M. P., Hanninen, T., Hallikainen, M., Alhainen, K., Iivonen, S., Mannermaa, A., Tuomilehto, J., Nissinen, A., and Soininen, H. (2002) *Ann. Intern. Med.* **137,** 149–155
22. Kuo, Y. M., Emmerling, M. R., Bisgaier, C. L., Essenburg, A. D., Lampert, H. C., Drumm, D., and Roher, A. E. (1998) *Biochem. Biophys. Res. Commun.* **252,** 711–715
23. Hofman, A., Ott, A., Breteler, M. M., Bots, M. L., Slooter, A. J., van Harskamp, F., van Duijn, C. N., Van Broeckhoven, C., and Grobbee, D. E. (1997) *Lancet* **349,** 151–154
24. Honig, L. S., Tang, M. X., Albert, S., Costa, R., Luchsinger, J., Manly, J., Stern, Y., and Mayeux, R. (2003) *Arch. Neurol.* **60,** 1707–1712
25. Luchsinger, J. A., Tang, M. X., Stern, Y., Shea, S., and Mayeux, R. (2001) *Am. J. Epidemiol.* **154,** 635–641
26. McIlroy, S. P., Dynan, K. B., Lawson, J. T., Patterson, C. C., and Passmore, A. P. (2002) *Stroke* **33,** 2351–2356
27. Knebl, J., DeFazio, P., Clearfield, M. B., Little, L., McConathy, W. J., McPherson, R., and Lacko, A. G. (1994) *Mech. Ageing Dev.* **73,** 69–77
28. Wolozin, B., Kellman, W., Ruosseau, P., Celesia, G. G., and Siegel, G. (2000) *Arch. Neurol.* **57,** 1439–1443
29. Jick, H., Zornberg, G. L., Jick, S. S., Seshadri, S., and Drachman, D. A. (2000) *Lancet* **356,** 1627–1631
30. Werner, N., Nickenig, G., and Laufs, U. (2002) *Basic Res. Cardiol.* **97,** 105–116
31. Mason, J. C. (2003) *Clin. Sci.* (*Lond.*) **105,** 251–266
32. Bi, X., Baudry, M., Liu, J., Yao, Y., Fu, L., Brucher, F., and Lynch, G. (2004) *J. Biol. Chem.* **279,** 48238–48245
33. Kato, T., Hashikabe, H., Iwata, C., Akimoto, K., and Hattori, Y. (2004) *Biochim. Biophys. Acta* **1689,** 267–272
34. Simons, M., Keller, P., De Strooper, B., Beyreuther, K., Dotti, C. G., and Simons, K. (1998) *Proc. Natl. Acad. Sci. U. S. A.* **95,** 6460–6464
35. Frears, E. R., Stephens, D. J., Walters, C. E., Davies, H., and Austen, B. M. (1999) *Neuroreport* **10,** 1699–1705
36. Buxbaum, J. D., Geoghagen, N. S., and Friedhoff, L. T. (2001) *J. Alzheimers Dis.* **3,** 221–229
37. Fassbender, K., Simons, M., Bergmann, C., Stroick, M., Lutjohann, D., Keller, P., Runz, H., Kuhl, S., Bertsch, T., von Bergmann, K., Hennerici, M., Beyreuther, K., and Hartmann, T. (2001) *Proc. Natl. Acad. Sci. U. S. A.* **98,** 5856–5861
38. Kojro, E., Gimpl, G., Lammich, S., Marz, W., and Fahrenholz, F. (2001) *Proc. Natl. Acad. Sci. U. S. A.* **98,** 5815–5820
39. Ehehalt, R., Keller, P., Haass, C., Thiele, C., and Simons, K. (2003) *J. Cell Biol.* **160,** 113–123
40. Bodovitz, S., and Klein, W. L. (1996) *J. Biol. Chem.* **271,** 4436–4440
41. Racchi, M., Baetta, R., Salvietti, N., Ianna, P., Franceschini, G., Paoletti, R., Fumagalli, R., Govoni, S., Trabucchi, M., and Soma, M. (1997) *Biochem. J.* **322,** 893–898
42. Galbete, J. L., Martin, T. R., Peressini, E., Modena, P., Bianchi, R., and Forloni, G. (2000) *Biochem. J.* **348,** 307–313
43. Puglielli, L., Konopka, G., Pack-Chung, E., Ingano, L. A., Berezovska, O., Hyman, B. T., Chang, T. Y., Tanzi, R. E., and Kovacs, D. M. (2001) *Nat. Cell Biol.* **3,** 905–912
44. Runz, H., Rietdorf, J., Tomic, I., de Bernard, M., Beyreuther, K., Pepperkok, R., and Hartmann, T. (2002) *J. Neurosci.* **22,** 1679–1689
45. Burns, M., Gaynor, K., Olm, V., Mercken, M., LaFrancois, J., Wang, L., Mathews, P. M., Noble, W., Matsuoka, Y., and Duff, K. (2003) *J. Neurosci.* **23,** 5645–5649
46. Jin, L. W., Maezawa, I., Vincent, I., and Bird, T. (2004) *Am. J. Pathol.* **164,** 975–985
47. Yamazaki, T., Chang, T. Y., Haass, C., and Ihara, Y. (2001) *J. Biol. Chem.* **276,** 4454–4460

48. Ross, S. L., Martin, F., Simonet, L., Jacobsen, F., Deshpande, R., Vassar, R., Bennett, B., Luo, Y., Wooden, S., Hu, S., Citron, M., and Burgess, T. L. (1998) *J. Biol. Chem.* **273,** 15309–15312
49. He, T.-C., Zhou, S., da Costa, L. T., Yu, J., Kinzler, K. W., and Vogelstein, B. (1998) *Proc. Natl. Acad. Sci. U. S. A.* **95,** 2509–2514
50. Goslin, K., and Banker, G. A. (1991) *Rat Hippocampal Neurons in Low Density Culture*, MIT Press, Cambridge, MA
51. Hsiao, K. K., Borchelt, D. R., Olson, K., Johannsdottir, R., Kitt, C., Yunis, W., Xu, S., Eckman, C., Younkin, S., Price, D., Iadecole, C., Clark, H. B., and Carlson, G. (1995) *Neuron* **15,** 1203–1218
52. Meske, V., Albert, F., Richter, D., Schwarze, J., and Ohm, T. G. (2003) *Eur. J. Neurosci.* **17,** 93–102
53. Heider, J. G., and Boyett, R. L. (1978) *J. Lipid Res.* **19,** 514–518
54. Brown, M. S., and Goldstein, J. L. (1980) *J. Lipid Res.* **21,** 505–517
55. Goldstein, J. L., and Brown, M. S. (1990) *Nature* **343,** 425–430
56. Keller, P., and Simons, K. (1998) *J. Cell Biol.* **140,** 1357–1367
57. Rodal, S. K., Skretting, G., Garred, O., Vilhardt, F., van Deurs, B., and Sandvig, K. (1999) *Mol. Biol. Cell* **10,** 961–974
58. Slunt, H. H., Thinakaran, G., Von Koch, C., Lo, A. C., Tanzi, R. E., and Sisodia, S. S. (1994) *J. Biol. Chem.* **269,** 2637–2644
59. Oltersdorf, T., Ward, P. J., Henriksson, T., Beattie, E. C., Neve, R., Lieberburg, I., and Fritz, L. C. (1990) *J. Biol. Chem.* **265,** 4492–4497
60. Nordstedt, C., Gandy, S. E., Alafuzoff, I., Caporaso, G. L., Iverfeldt, K., Grebb, J. A., Winblad, B., and Greengard, P. (1991) *Proc. Natl. Acad. Sci. U. S. A.* **88,** 8910–8914
61. Hsiao, K., Chapman, P., Nilsen, S., Eckman, C., Harigaya, Y., Younkin, S., Yang, F., and Cole, G. (1996) *Science* **274,** 99–103
62. Kim, S. H., Yin, Y. I., Li, Y. M., and Sisodia, S. S. (2004) *J. Biol. Chem.* **279,** 48615–48619
63. Skovronsky, D. M., Doms, R. W., and Lee, V. M. (1998) *J. Cell Biol.* **141,** 1031–1039
64. Vicent, D., Maratos-Flier, E., and Kahn, C. R. (2000) *Mol. Cell. Biol.* **20,** 2158–2166
65. Ridley, A. J. (2001) *Traffic* **2,** 303–310
66. Farnsworth, C. C., Gelb, M. H., and Glomset, J. A. (1990) *Science* **247,** 320–322
67. Epstein, W. W., Lever, D., Leining, L. M., Bruenger, E., and Rilling, H. C. (1991) *Proc. Natl. Acad. Sci. U. S. A.* **88,** 9668–9670
68. Rilling, H. C., Breunger, E., Epstein, W. W., and Crain, P. F. (1990) *Science* **247,** 318–320
69. Dugan, J. M., deWit, C., McConlogue, L., and Maltese, W. A. (1995) *J. Biol. Chem.* **270,** 10982–10989
70. McConlogue, L., Castellano, F., deWit, C., Schenk, D., and Maltese, W. A. (1996) *J. Biol. Chem.* **271,** 1343–1348
71. Cordy, J., M., Hussain, I., Dingwall, C., Hooper, N. M., and Turner, A. J. (2003) *Proc. Natl. Acad. Sci. U. S. A.* **100,** 11735–11740